

2

NAVAL POSTGRADUATE SCHOOL

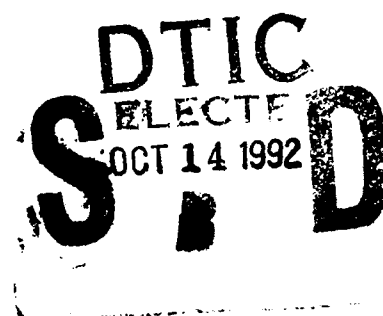
Monterey, California

AD-A256 085

1



Original contains color
plates: All DTIC reproductions
will be in black and
white



THESIS

SATELLITE DETECTION OF COMPLEX AEROSOLS
OVER
THE ARABIAN PENINSULA/GULF

by

William P. Morgan

March, 1992

Thesis Advisor:

Philip A. Durkee

Approved for public release; distribution is unlimited

92-27041



118
pgs

DISCLAIMER NOTICE



THIS DOCUMENT IS BEST QUALITY AVAILABLE. THE COPY FURNISHED TO DTIC CONTAINED A SIGNIFICANT NUMBER OF COLOR PAGES WHICH DO NOT REPRODUCE LEGIBLY ON BLACK AND WHITE MICROFICHE.

REPORT DOCUMENTATION PAGE				
1a. REPORT SECURITY CLASSIFICATION Unclassified			1b. RESTRICTIVE MARKINGS	
2a. SECURITY CLASSIFICATION AUTHORITY			3. DISTRIBUTION/AVAILABILITY OF REPORT Approved for public release; distribution is unlimited.	
2b. DECLASSIFICATION/DOWNGRADING SCHEDULE				
4. PERFORMING ORGANIZATION REPORT NUMBER(S)			5. MONITORING ORGANIZATION REPORT NUMBER(S)	
6a. NAME OF PERFORMING ORGANIZATION Naval Postgraduate School		6b. OFFICE SYMBOL (If applicable) 55	7a. NAME OF MONITORING ORGANIZATION Naval Postgraduate School	
6c. ADDRESS (City, State, and ZIP Code) Monterey, CA 93943-5000			7b. ADDRESS (City, State, and ZIP Code) Monterey, CA 93943-5000	
8a. NAME OF FUNDING/SPONSORING ORGANIZATION		8b. OFFICE SYMBOL (If applicable)	9. PROCUREMENT INSTRUMENT IDENTIFICATION NUMBER	
8c. ADDRESS (City, State, and ZIP Code)			10. SOURCE OF FUNDING NUMBERS	
			Program Element No.	Project No.
			Task No.	Work Unit Accession Number
11. TITLE (Include Security Classification) SATELLITE DETECTION OF COMPLEX AEROSOLS OVER THE ARABIAN PENINSULA/GULF				
12. PERSONAL AUTHOR(S) Morgan, William P.				
13a. TYPE OF REPORT Master's Thesis		13b. TIME COVERED From To	14. DATE OF REPORT (year, month, day) 1992 March	15. PAGE COUNT 116
16. SUPPLEMENTARY NOTATION The views expressed in this thesis are those of the author and do not reflect the official policy or position of the Department of Defense or the U.S. Government.				
17. COSATI CODES			18. SUBJECT TERMS (continue on reverse if necessary and identify by block number)	
FIELD	GROUP	SUBGROUP	Aerosol Detection, Scatter Plot, Mask	
19. ABSTRACT (continue on reverse if necessary and identify by block number) Satellite detection of complex aerosols, in particular, oil smoke over water and dust over land, is generally difficult. On 1 March 1991, a smoke plume generated by burning Kuwaiti oil wells and a dust storm over the southwestern Arabian peninsula, provided the opportunity to study both of these effects. Utilizing NOAA-11 data, a two dimensional scatter plot analysis technique was employed to determine and classify the radiative signatures of the smoke and dust. A two dimensional mask routine was then used to assess the reliability of the scatter plot analyses and spatially display the results. A channel 1 to channel 2 radiance ratio versus a channel 4 brightness temperature combination provided the best separation of the smoke signature from water. The dust plume was unambiguously represented by a channel 4 brightness temperature minus channel 5 brightness temperature image versus a channel 4 brightness temperature combination. Together the 2D scatter plot technique and 2D mask form the groundwork for a possible detection algorithm.				
20. DISTRIBUTION/AVAILABILITY OF ABSTRACT <input checked="" type="checkbox"/> UNCLASSIFIED/UNLIMITED <input type="checkbox"/> SAME AS REPORT <input type="checkbox"/> DTIC USERS			21. ABSTRACT SECURITY CLASSIFICATION Unclassified	
22a. NAME OF RESPONSIBLE INDIVIDUAL Philip A. Durkee			22b. TELEPHONE (Include Area code) 408-646-3465	22c. OFFICE SYMBOL MR/De

Approved for public release; distribution is unlimited.

**Satellite Detection Of Complex Aerosols
Over The Arabian Peninsula/Gulf**

by

**William P. Morgan
Lieutenant Commander, United States Navy
B.S., United States Naval Academy, 1981**

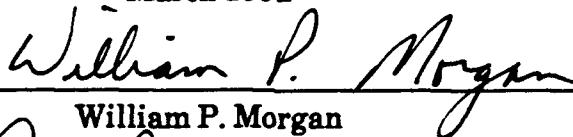
**Submitted in partial fulfillment
of the requirements for the degree of**

MASTER OF SCIENCE IN METEOROLOGY AND OCEANOGRAPHY

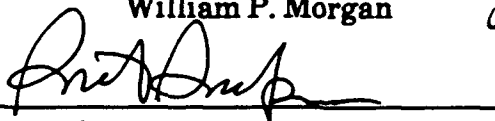
from the

**NAVAL POSTGRADUATE SCHOOL
March 1992**

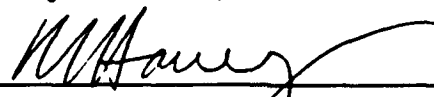
Author:


William P. Morgan

Approved by:


Philip A. Durkee, Thesis Advisor


Carlyle A. Wash, Second Reader


Robert L. Haney, Chairman
Department of Meteorology

ABSTRACT

Satellite detection of complex aerosols, in particular, oil smoke over water and dust over land, is generally difficult. On 1 March 1991, a smoke plume generated by burning Kuwaiti oil wells and a dust storm over the southwestern Arabian Peninsula, provide the opportunity to study both of these effects. Utilizing NOAA-11 AVHRR data, a two dimensional scatter plot analysis technique was employed to determine and classify the radiative signatures of the smoke and dust. A two dimensional mask routine was then used to assess the reliability of the scatter plot analyses and spatially display the results. A channel 1 to channel 2 radiance ratio and a channel 4 brightness temperature combination provided the best separation of the smoke signature from water. The dust plume was unambiguously represented by a channel 5 brightness temperature minus channel 4 brightness temperature image and a channel 4 brightness temperature combination. Together the 2D scatter plot technique and 2D mask form the groundwork for a possible detection algorithm.

iii

DTIC QUALITY INSPECTED 1

Accession For	
NTIS GRA&I	<input checked="" type="checkbox"/>
DTIC TAB	<input type="checkbox"/>
Unannounced	<input type="checkbox"/>
Justification	
By	
Distribution/	
Availability Codes	
Dist.	Avail and/or Special
A-1	

TABLE OF CONTENTS

I.	INTRODUCTION	1
A.	MOTIVATION	1
B.	GOALS	2
II.	BACKGROUND	5
A.	BASIC THEORY	5
B.	CHARACTERISTICS OF OIL SMOKE	6
C.	CHARACTERISTICS OF DESERT DUST	7
D.	1 MARCH 1991 SMOKE/DUST PLUME DISTRIBUTION	7
	1. Smoke Plume	7
	2. Dust Plume	13
III.	PROCEDURES	15
A.	DATA	15
B.	SATELLITE DATA PROCESSING	16
C.	DATA ANALYSIS	17
	1. Radiative Signature Analysis	17
	a. Derived Parameters	17
	b. Scatter Plot Technique	18
	c. Verification of Radiative Signature Analyses	24

IV. SCATTER PLOT ANALYSES/RESULTS	28
A. UPPER GULF SCATTER PLOTS	28
1. Case 1 Scatter Plot Analysis: S12L Versus	
Temp 4 (Figure 17)	33
a. Water:	33
b. Thick Smoke:	36
c. Thin Smoke Over Land:	37
d. Thin Smoke Over Water:	38
e. Land:	38
f. Summary:	39
2. Case 2 Scatter Plot Analysis: Cal 2 Versus	
Temp 4 (Figure 18)	40
a. Water:	40
b. Thick Smoke:	42
c. Thin Smoke Over Land:	42
d. Thin Smoke Over Water:	42
e. Land:	43
f. Summary:	43
3. Case 3 Scatter Plot Analysis: T3-T4 Versus	
Temp 4 (Figure 20)	45
a. Water:	45
b. Thick Smoke:	47
c. Thin Smoke Over Land:	49
d. Thin Smoke Over Water:	50
e. Land:	51
f. Summary	51

4. Case 4 Scatter Plot Analysis: T3-T4 versus	
Cal 2 (Figure 22)	52
a. Water:	54
b. Thick Smoke:	54
c. Thin Smoke Over Land:	55
d. Thin Smoke Over Water:	55
e. Land:	56
f. Summary:	56
B. ARABIAN PENINSULA SCATTER PLOTS	57
1. Case 1 Scatter Plot Analysis: Cal 2 versus	
Temp 3 (Figure 24)	59
a. Dust:	59
b. High Dust:	61
c. Smoke:	62
d. Smoke/Dust Mixed:	62
e. Summary:	62
2. Case 2 Scatter Plot Analysis: Cal 2 versus	
Temp 4 Figure 25)	63
a. Dust:	63
b. High dust:	65
c. Smoke:	67
d. Smoke/Dust Mixed:	67
e. Summary:	67
3. Case 3 Scatter Plot Analysis: Cal 2 Versus	
Temp 5 (Figure 27)	68
a. Dust:	68

b. High Dust:	69
c. Smoke:	69
d. Smoke/Dust Mixed:	72
e. Summary:	72
4. Case 4 Scatter Plot Analysis: Cal 2 versus	
T4-T5 (Figure 29)	72
a. Dust:	74
b. High Dust:	74
c. Smoke:	74
d. Smoke/Dust Mixed:	74
e. Summary:	75
5. Case 5 Scatter Plot Analysis: T3-T4 versus	
Cal 2 (Figure 30)	75
a. Dust:	75
b. High Dust:	77
c. Smoke:	77
d. Smoke/Dust Mixed:	77
e. Summary:	77
6. Case 6 Scatter Plot Analysis: T4-T5 versus	
Temp 4 (Figure 31)	78
C. VERIFICATION OF SCATTER PLOT ANALYSES	80
1. Upper Gulf Scatter Plots	80
a. S12L versus Temp 4	80
b. T3-T4 versus Temp 4	82
2. Arabian Peninsula Scatter Plots	86
a. Cal 2 versus Temp 5	86

b. Cal 2 versus T4-T5	86
c. T4-T5 versus Temp 4	92
V. CONCLUSIONS AND RECOMMENDATIONS	98
A. SMOKE RADIATIVE SIGNATURE	98
B. DUST RADIATIVE SIGNATURE	99
C. TWO DIMENSIONAL MASK AND SCATTER PLOT TECHNIQUE	99
D. RECOMMENDATIONS	100
LIST OF REFERENCES	102
INITIAL DISTRIBUTION LIST	103

LIST OF TABLES

Table 1.	AVHRR/1 AND 2 CHANNEL BANDWIDTHS	16
----------	----------------------------------	----

LIST OF FIGURES

Figure 1. 1 March 1991 1026 UTC visible satellite image of Arabian Peninsula/Gulf.	3
Figure 2. Distribution of imaginary index of refraction for desert aerosols	8
Figure 3. Enlargement of Figure 2	9
Figure 4. 1 March 1991 0900 UTC surface pressure analysis	11
Figure 5. 1 March 1991 00 UTC Dharhan, Saudi Arabia sounding.	12
Figure 6. 1 March 1991 12 UTC Riyadh, Saudi Arabia sounding.	14
Figure 7. Procedural flow chart for producing full image 2D scatter plot for two subimages.	19
Figure 8. Example of full image 2D scatter plot . . .	21
Figure 9. Procedural flow chart for producing image sample areas on 2D scatter plot	22
Figure 10. Example of single feature 2D scatter plot.	23
Figure 11. Procedural flow chart for verification of radiative signature analyses.	25
Figure 12. Same as Figure 8 except example of analyzed 2D signature limits on full image 2D scatter plot	26

Figure 15.	1 March 1991 1026 UTC Upper Gulf S12L image depicting feature sample areas	31
Figure 16.	1 March 1991 1026 UTC AVHRR Temp 4 satellite image	32
Figure 17.	Case 1 Upper Gulf scatter plot.	34
Figure 18.	Case 2 Upper Gulf scatter plot.	41
Figure 19.	1 March 1991 1026 UTC Upper Gulf Cal 2 image.	44
Figure 20.	Case 3 Upper Gulf scatter plot.	46
Figure 21.	1 March 1991 1026 UTC T3-T4 Upper Gulf image.	48
Figure 22.	Case 4 Upper Gulf scatter plot.	53
Figure 23.	1 March 1991 1026 UTC Temp 4 Arabian Peninsula image depicting feature sample areas	58
Figure 24.	Case 1 Arabian Peninsula scatter plot. . .	60
Figure 25.	Case 2 Arabian Peninsula scatter plot. . .	65
Figure 26.	Normalized Planck curves representing solar radiation	66
Figure 27.	Case 3 Arabian Peninsula scatter plot. . .	70
Figure 28.	Infrared water vapor (H ₂ O) transmittance. .	71
Figure 29.	Case 4 Arabian Peninsula scatter plot. . .	73
Figure 30.	Case 5 Arabian Peninsula scatter plot. . .	76
Figure 31.	Case 6 Arabian Peninsula scatter plot. . .	79
Figure 32.	Analyzed 2D feature radiative signature limits for case 1 Upper Gulf scatter plot.	81
Figure 33.	S12L versus Temp 4 mask	83

Figure 33. S12L versus Temp 4 mask	83
Figure 34. Analyzed 2D feature radiative signatures .	84
Figure 35. T3-T4 versus Temp 4 mask utilizing limitations	85
Figure 36. Analyzed 2D "dust" radiative signature . .	87
Figure 37. Cal 2 versus Temp 5 mask utilizing limits .	88
Figure 38. Cal 2 1 March 1991 1026 UTC Arabian Peninsula image.	89
Figure 39. Temp 5 1 March 1991 1026 UTC Arabian Peninsula image.	90
Figure 40. Analyzed 2D "dust" radiative signature for case 4 Arabian Peninsula scatter plot.	91
Figure 41. Cal 2 1 March 1991 1026 UTC satellite image.	93
Figure 42. T4-T5 1 March 1991 1026 UTC satellite image.	94
Figure 43. Cal 2 versus T4-T5 mask utilizing limits in Figure 40.	95
Figure 44. Analyzed 2D "dust" radiative signature for Case 6 Arabian Peninsula scatter plot.	96
Figure 45. T4-T5 versus Temp 4 mask utilizing limits in Figure 44.	97

ACKNOWLEDGEMENTS

I would like to thank my wife, Cheryl for her undying support and nimble typing fingers. Without her help I would still be typing. Thanks to my son, Kyle, and daughter, Lindsey, for understanding why "Daddy" was not able to spend as much time with them. Special thanks goes to Kurt Nielsen and Craig Motell for writing the all important Fortran programs necessary to complete this project and helping me keep a sense of humor - thanks guys for all your help! Thanks to Tom Lee at NRL and Dennis Laws at FNOC for the data support. And last but not least, thanks to Professor Durkee for his guidance, patience and open door.

I. INTRODUCTION

A. MOTIVATION

On 1 March 1991, the region of the Arabian Peninsula and Arabian Gulf presents a unique opportunity to remotely study the characteristics of two categories of complex aerosols: oil smoke and desert dust. A smoke plume is being produced by some 610 burning Kuwaiti oil wells ignited by the retreating Iraqi army during the recent Gulf War. Estimates by Johnson et al. (1991) put the total burn rate of the oil fires at 202.5 metric tons per year or 3.9 million barrels per day. Additionally, a dust storm on the southern Arabian Peninsula created a large dust plume with dimensions several hundreds of kilometers in length and width. The presence of these two types of aerosols in the same region on the same day offers an unparalleled "data rich" environment ideal for a study in satellite detection of complex aerosols.

Both military and scientific concerns motivate the need for accurate aerosol detection. First, aerosol concentrations can negatively impact military operations. They reduce visibilities, affect weapon, machine and human effectiveness and hamper aircraft/satellite intelligence gathering efforts vital to most military operations. Accurate real-time analyses of aerosol spatial distributions and concentrations

would be a valuable mission planning aid for all military commanders. Second, aerosols can effect changes in local, regional and in some cases the global environment. Some of these effects include sharp increases and decreases in surface and atmospheric heating rates, production of anomalous mesoscale weather features and long-term changes in climatology. Thus, knowing distributions and concentrations of aerosols can aid scientists in studying and predicting aerosol effects on the environment.

B. GOALS

The primary goal of this project is to accurately identify the radiative signatures for smoke and dust over the Arabian Gulf and Arabian Peninsula on 1 March 1991. To achieve this goal, a scatter plot analysis technique is employed. This technique is currently used for cloud classification wherein cloud type is identified by a combination of its IR brightness temperature and its solar reflectance. The actual detection and classification of smoke and dust, however, is complicated by the spectral radiative influence of atmospheric constituents (primarily water vapor), clouds and geographic features (land and water) on the aerosol radiative signatures. In particular, it is difficult to detect smoke over water and dust over land. Figure 1, a 1 March 1991 visible satellite image of the Arabian Peninsula/Gulf, demonstrates these difficult effects. Smoke being generated by the oil fires is

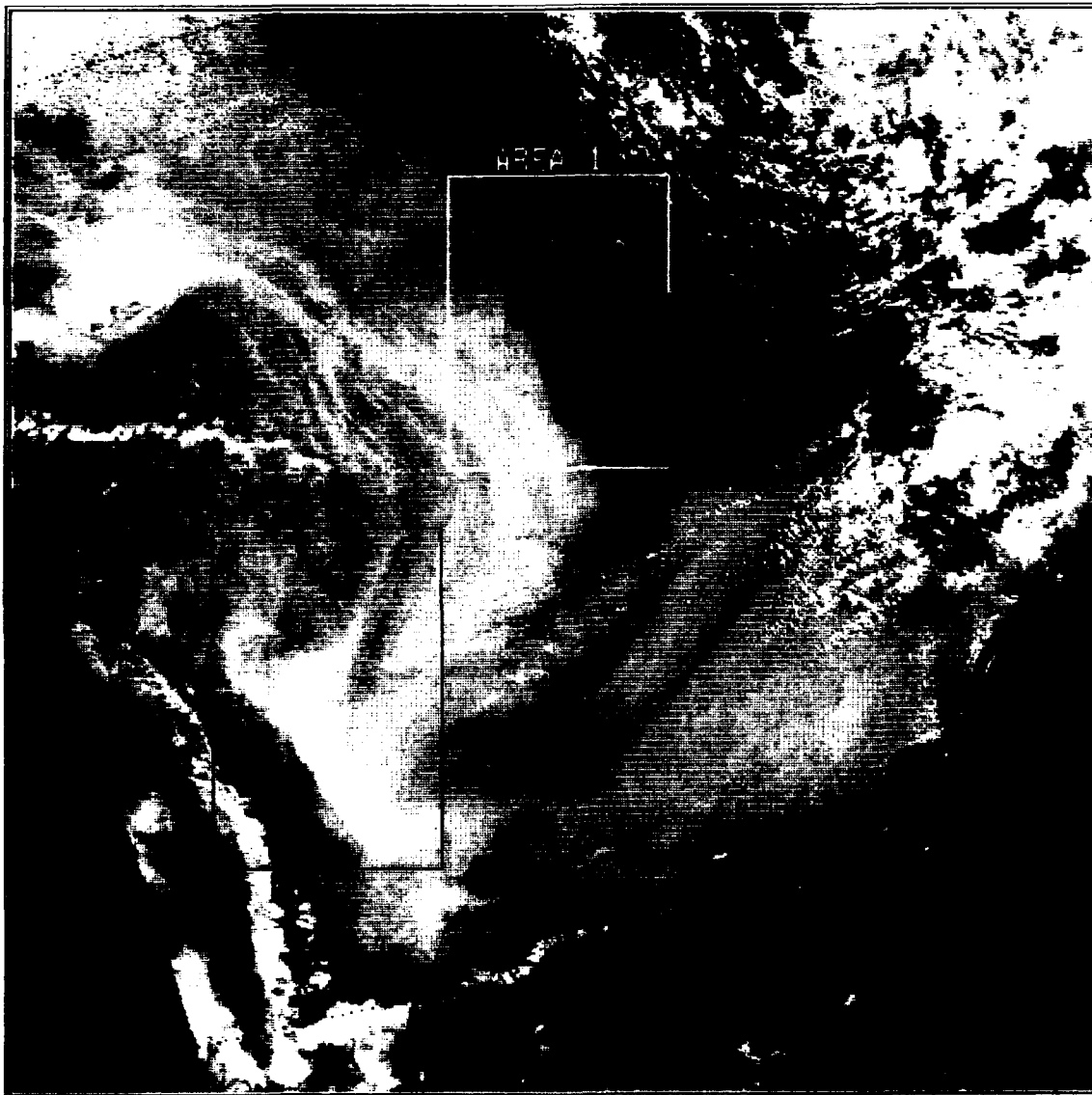


Figure 1. 1 March 1991 1026 UTC visible satellite image of Arabian Peninsula/Gulf. Smoke is nondiscernible over Gulf (Area 1). Dust plume is difficult to discern in Area 2.

discernible over land but not over the gulf (area 1) and the dust storm over the southern Arabian Peninsula (area 2) is barely discernible, if at all, from the surrounding desert. Therefore, a major challenge in this project is to determine the spectral radiance of aerosol particles and then isolate them using the scatter plot technique.

In addition to the primary goal, there are three secondary goals embedded in this project. The first is to evaluate the scatter plot analysis technique as to its viability for analyzing aerosol radiative signatures. Second, the project will evaluate the two dimensional masking routine as to its viability for representing and analyzing aerosol spatial distributions and concentrations. And third, these aerosol signatures will aid in development of an aerosol detection algorithm for possible military application.

II. BACKGROUND

A. BASIC THEORY

The theory behind this study is based on the fundamentals of radiative transfer. Simply by knowing what can happen to a photon in a medium (as a function of its wavelength) and what photons a satellite detects, one can understand the basis of the analyses.

A photon will either be absorbed by the medium, reflected by the medium or transmitted through the medium. Again, what happens depends on the wavelength of the photon and the physical characteristics of the medium. A satellite will detect photons reflected by the surface and/or aerosols or those emitted by the surface, aerosol and/or atmosphere. In either case, the number of photons detected is dependent upon the physical characteristics of the surface, aerosol and atmosphere as a function of wavelength (λ).

The following simple equation summarizes the satellite detection where L = monochromatic radiance:

$$L_{\text{satellite}}(\lambda) = L_{\text{surface}}(\lambda) + L_{\text{aerosol}}(\lambda) + L_{\text{atmosphere}}(\lambda)$$

Aerosols are detectable when the aerosol radiance contrast strongly with the ambient surface and/or atmospheric radiance.

B. CHARACTERISTICS OF OIL SMOKE

The Kuwaiti oil fires represent the first time a large scale oil smoke plume has been available for scientific research. Therefore, little is known about the actual radiative effects and characteristics of a smoke plume of this type. Laboratory experiments, however, have shown approximately 100% of aerosol from burned oil is elemental carbon (Crutzen et al., 1984). Elemental carbon is highly absorbent throughout the solar spectrum which is why oil smoke generally appears black at visible wavelengths (Turco et al., 1990). Additionally Turco et al. (1990) has noted that smoke radiative absorption decreases slowly with increasing wavelength.

Actual measurements of the Kuwaiti smoke plume, obtained by a British Meteorological Office Research flight on 18 March 1991, indicates near field particles are composed by spherical particles of approximately $1\mu\text{m}$ diameter formed into aggregates up to several micrometers in length/size (Johnson et al., 1991). Additionally, there is high near source water vapor content giving the potential for condensed water drops. The water vapor is a combustion byproduct as a result of water intrusion into the oil wells (Limaye et al., 1991). Finally, there are reports of oil drops in the near field plume.

C. CHARACTERISTICS OF DESERT DUST

A study by Carlson and Benjamin (1980) identified some general characteristics of dust. First, it is highly reflective through all visible wavelengths. Second, there is a general trend of increasing absorption with increasing wavelength from near IR into middle IR. This is indicated by Figure 2 which gives a distribution of the complex index of refraction for desert aerosols. Durkee (1984) provides a good discussion of how the imaginary index of refraction controls the absorption by particles. Finally there is a high variability in absorption in the IR water vapor window (8-12 microns). Figure 3, which is an enlargement of Figure 2, demonstrates this characteristic. Notice the variability between the channel 4 and 5 wavelength bands. Dust absorbs channel 4 wavelengths better than channel 5. This is an important characteristic for dust detection in this study.

D. 1 MARCH 1991 SMOKE/DUST PLUME DISTRIBUTION

1. Smoke Plume

There are two layers of smoke as a result of the Kuwaiti oil fires. A low level smoke plume is being advected southeastward over the Gulf and along the Saudi Arabian coast. In the vicinity of Qatar, the plume is turned and advected inland over Saudi Arabia. This was determined by analyses of various AVHRR passes along with surface and upper air wind

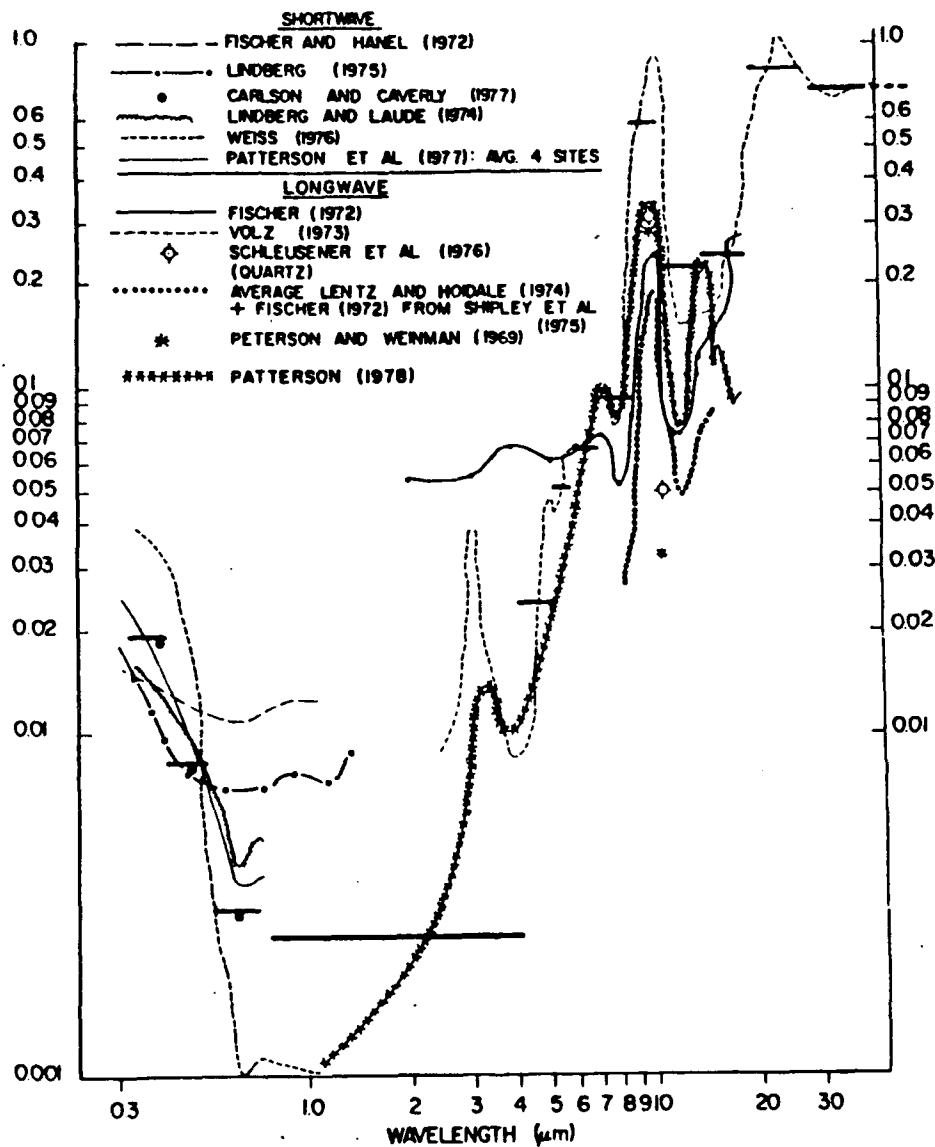


Figure 2. Distribution of imaginary index of refraction for desert aerosols, from Carlson and Benjamin (1980).

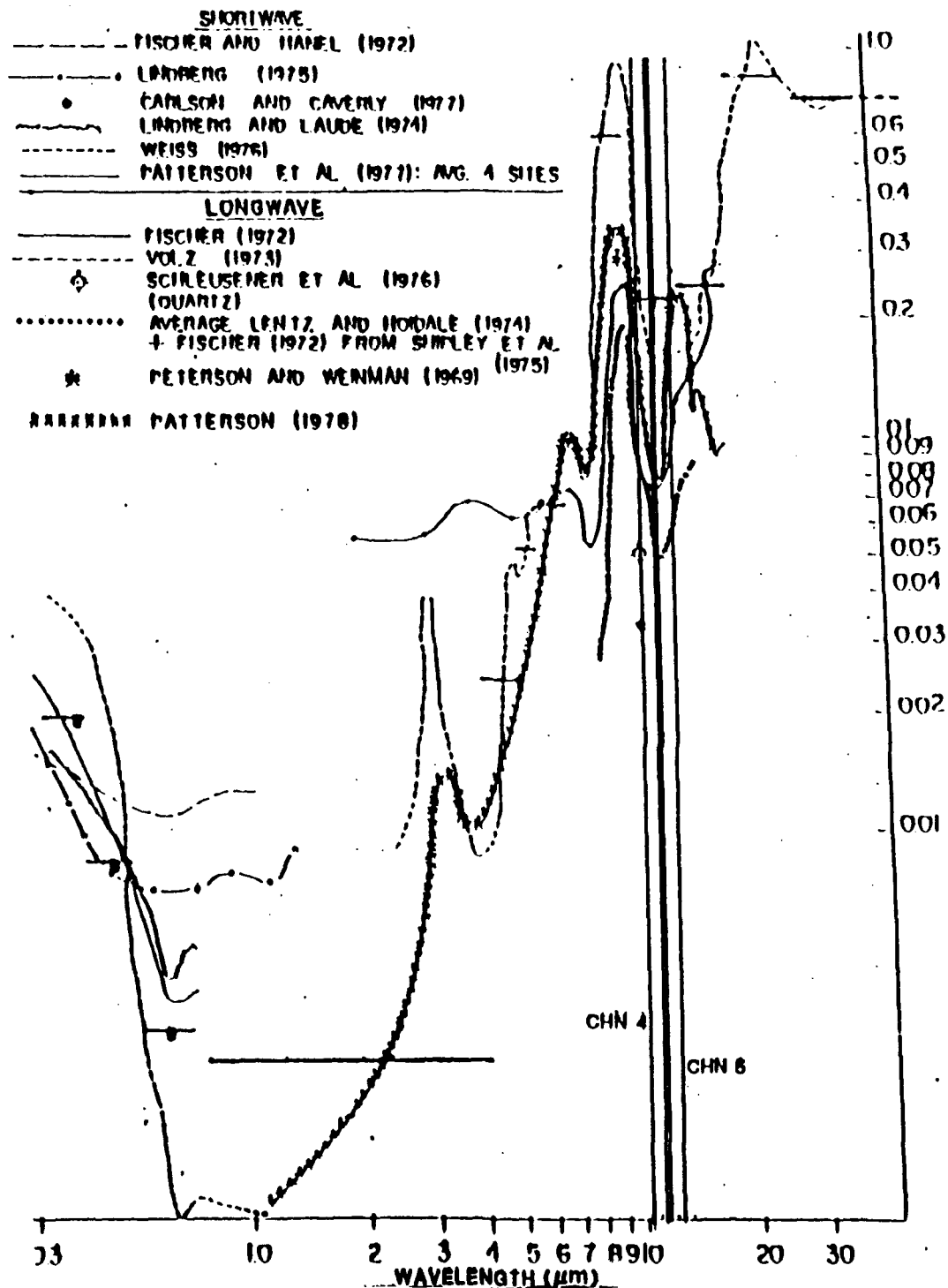


Figure 3. Enlargement of Figure 2 except with AVHRR channels 4 and 5 wavelength bands indicated. Note generally higher imaginary index of refraction for channel 4 wavelength.

and pressure fields. The weather data was obtained from Fleet Numerical Oceanography Center (FNOC). Figure 4 shows the 0900 UTC surface pressure analysis and surface wind observations which support the advection pattern. The top of the low level plume is between 1650 and 2115 meters. This was crudely determined utilizing the 1 March 1991 00 UTC Dharhan, Saudi Arabia sounding, Figure 5, (location on Dharhan provided later in Figure 13) along with a 1 March 1991, 0352 UTC channel 4 brightness temperature image. Essentially, a temperature range for the plume tops was extracted from the brightness temperature images and plotted on the sounding temperature profile. The plotted temperature correspond to a particular height in millibars which was converted to meters. The estimated altitude range falls within the observed smoke layer range of 1000 to 3000 meters as reported by Limaye et al. (1991). The data for the Limaye et al. study was taken on 18 March 1991 under similar meteorological conditions as on 1 March.

An upper level smoke layer between 3600 and 4200 meters is advected eastward over the Gulf and towards Iran. This correlates well with strong westerly winds 700 millibars and above as indicated in Figure 5. The altitude range of this upper level smoke plume was not determined in the project, but comes from the reported observations in the Limaye et al. (1991) study.

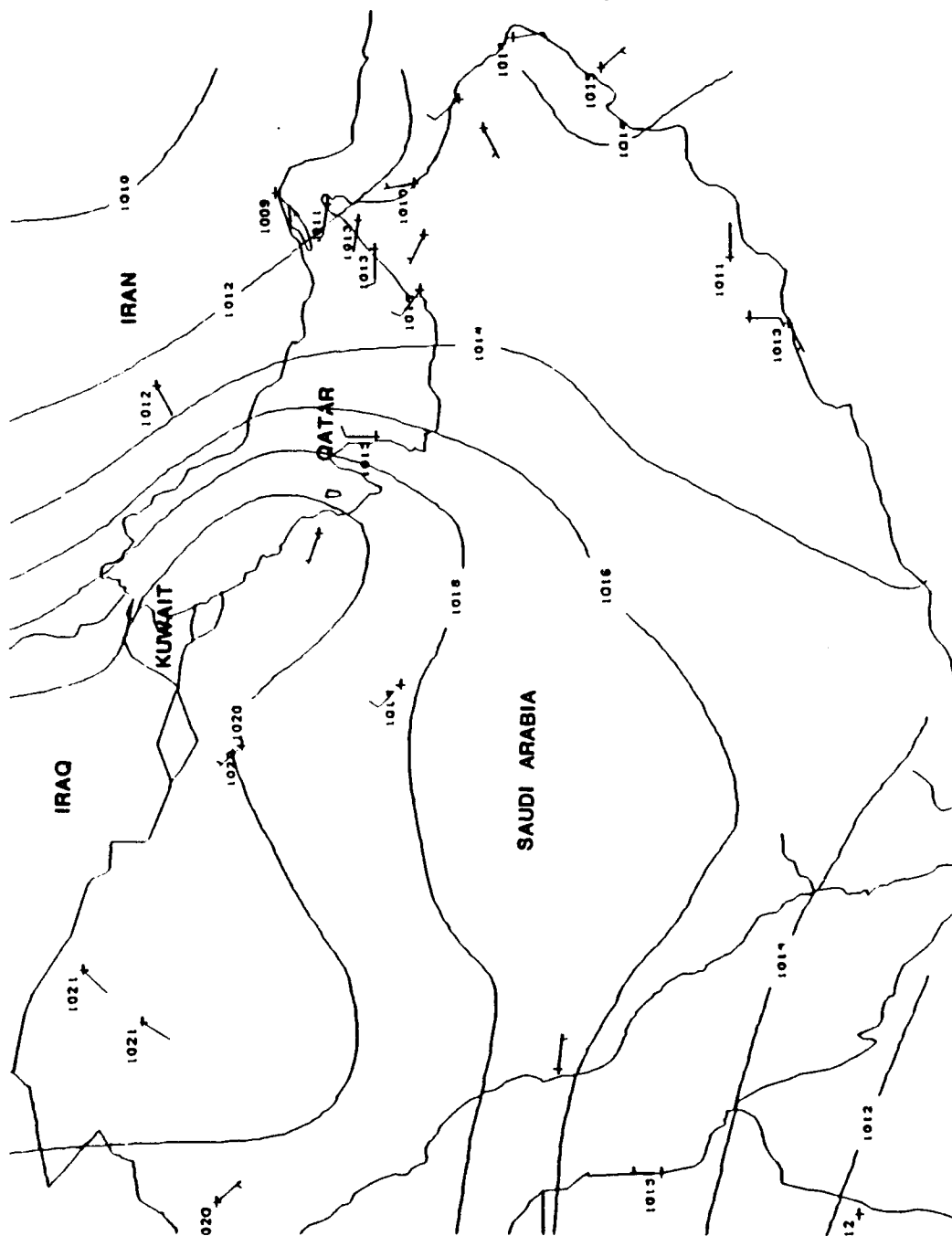


Figure 4. 1 March 1991 0900 UTC surface pressure analysis in millibars and station surface winds in knots.

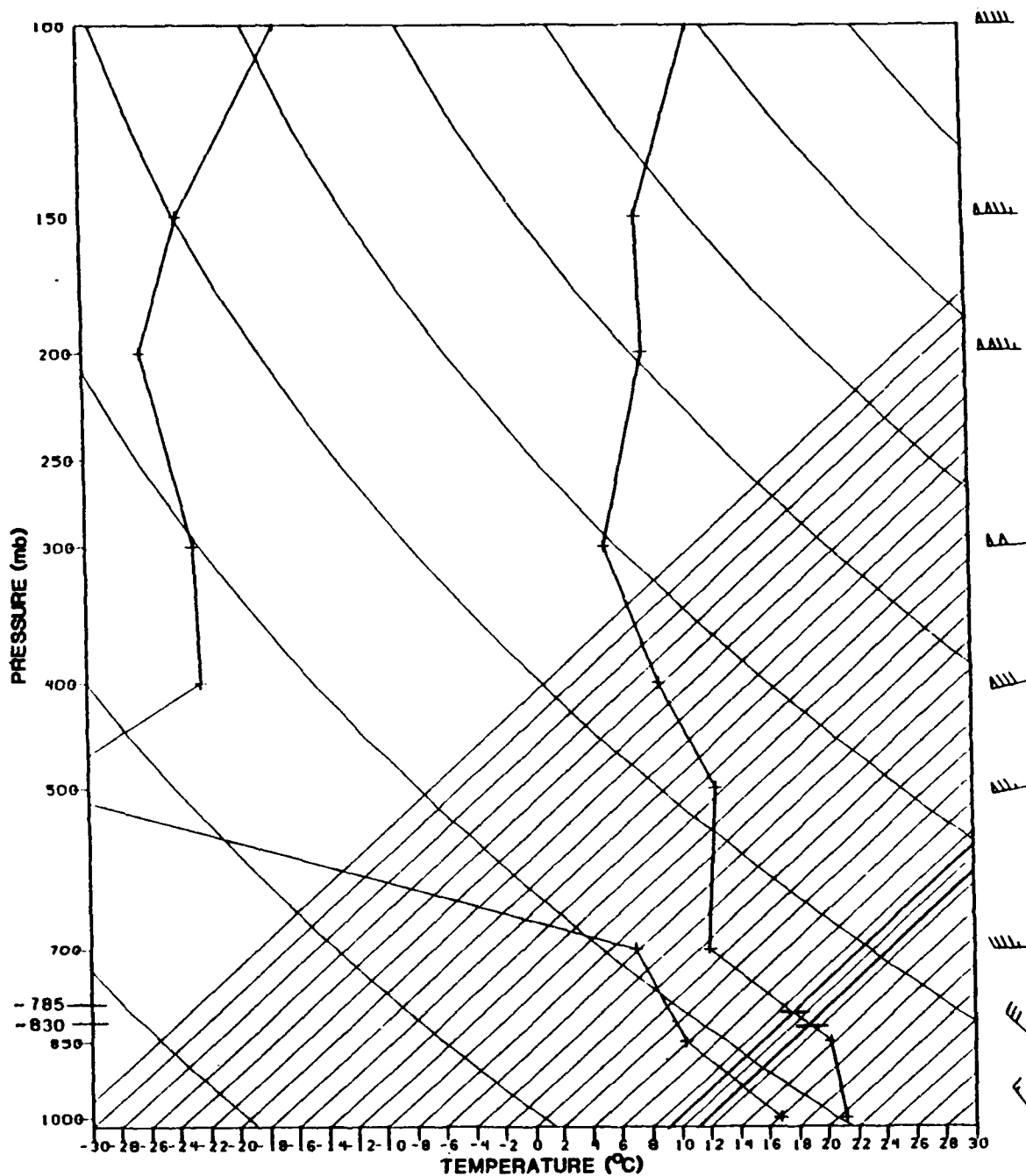


Figure 5. 1 March 1991 00 UTC Dharhan, Saudi Arabia sounding. Used to determine low level smoke plume between 830mb to 785mb or approximately 1650m to 2115m.

2. Dust Plume

The dust plume has its source approximately 335km south southeast of Riyadh, Saudi Arabia. The plume is advected southwestward approximately 515km to the base of the Hejaz Asir mountains. This advection is supported by the surface pressure pattern seen in Figure 4. The dust cloud then spreads some 600-700km along the base of the mountains. Tops of the dust plume range from 3000 to 4000 meters. The tops were determined in the same way as the low level smoke plume except the 1 March 1991 12 UTC Riyadh, Saudi Arabia sounding, Figure 6, and a 1 March 1991 1026 UTC channel 4 brightness temperature image were used.

•

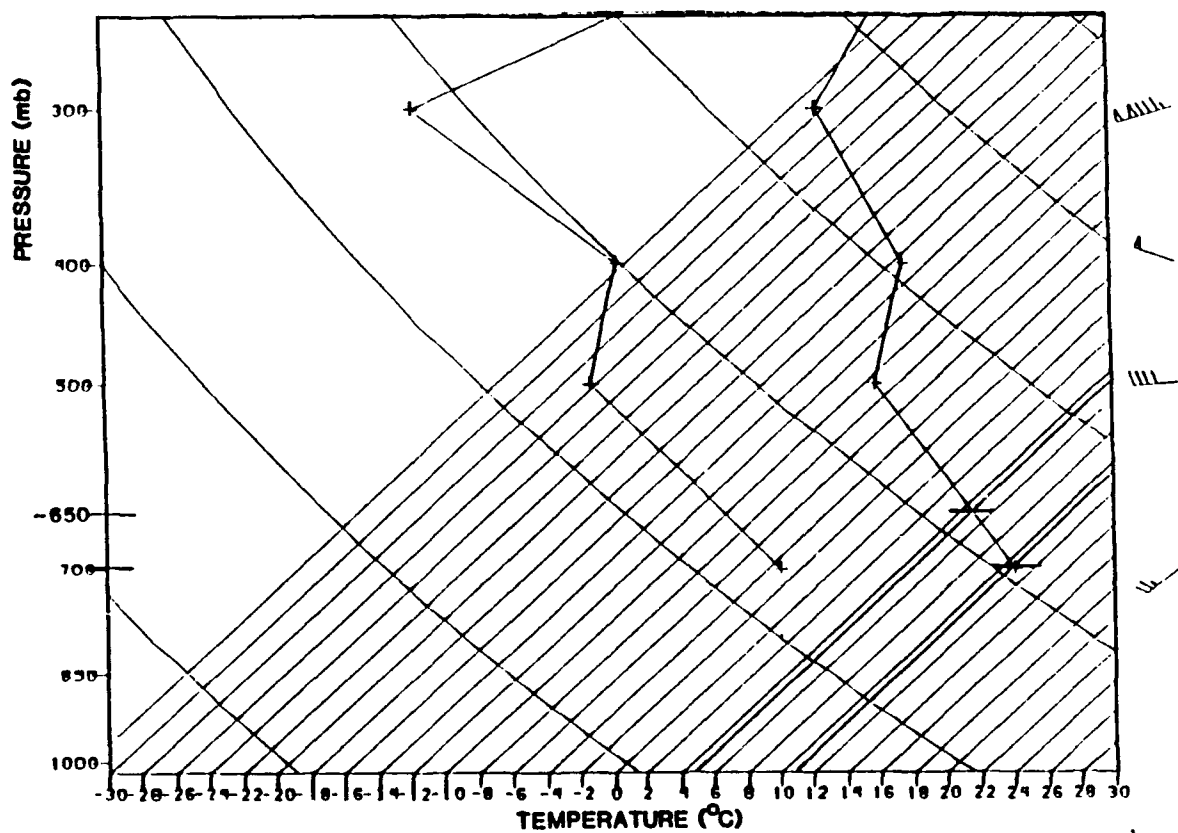


Figure 6. 1 March 1991 12 UTC Riyadh, Saudi Arabia sounding. Used to determine dust plume top between 700mb and 650mb or approximately 3000m to 4000m.

III. PROCEDURES

A. DATA

Satellite data used in this project was collected by the National Oceanographic and Atmospheric Administration (NOAA) 10 and 11 sun synchronous polar orbiting satellites. The NOAA 10 data was taken on 1 March 1991 at 0352 UTC (0652 local) in a descending node over the Middle East and the NOAA 11 data was taken on 1 March 1991 at 1026 UTC (1426 local) in an ascending node over the Middle East. Both the NOAA 10 and 11 data are contained on National Environmental Satellite Data and Information Service (NESDIS) tapes obtained from the Navy Oceanographic and Atmospheric Research Lab West (NOARL West). Advanced Very High Resolution Radiometer (AVHRRs) measured the upwelled radiance. AVHRR/1 on NOAA 10 has four channels or spectral bands and the AVHRR/2 on the NOAA 11 satellite has 5 channels. Table 1 indicates the bandwidth of the two radiometers.

NOAA 10 data was used to determine the approximate vertical extent of the low level smoke plume. NOAA 11 data was used to derive parameters for all scatter plots and to determine the vertical extent of the dust plume.

Table 1. AVHRR/1 AND 2 CHANNEL BANDWIDTHS (ADAPTED FROM KIDDER AND VONDER HAAR, 1992)

CHANNEL	AVHRR/1 BW	AVHRR/2 BW	RADIANCE
1	.55-.68 μ m	.58-.68 μ m	Red Visible
2	.75-1.10 μ m	.725-1.10 μ m	Near IR
3	3.55-3.93 μ m	3.55-3.93 μ m	Middle IR
4	10.5-11.5 μ m	10.3-11.3 μ m	Thermal IR
5	Channel 4 Repeated	11.5-12.5 μ m	Thermal IR

B. SATELLITE DATA PROCESSING

All processing was performed in the Interactive Digital Environmental Analysis Laboratory (IDEA Lab) at the Naval Postgraduate School (NPS) in Monterey, California. Initial satellite data processing utilized two IDEA Lab programs. AVIAN 3.0 written by Motell et al., (1991) was used to glean tapes and produce desired satellite parameters/images from satellite overviews. And DIPS, a program designed to work with existing satellite images, was used to perform enhancements and annotate on images. DIPS is essentially a "finishing" program for satellite images. The TEKTRONIX RGB color printer was utilized for all image reproduction via the IDEA Lab workstations.

C. DATA ANALYSIS

1. Radiative Signature Analysis

Seven parameters/images are derived from the NOAA 11 AVHRR/1 to assist in analyzing feature signatures. A two dimensional scatter plot analysis technique is then employed to analyze the individual signatures. After the feature signatures are determined, a two dimensional mask program is used to spatially display the results of the analyses and assess their reliability.

a. Derived Parameters

The following seven parameters are utilized in this project:

1. Channel 2 calibrated albedo (Cal 2)
2. Channel 1/Channel 2 radiance ratio (S12L)
3. Channel 3 Brightness Temperature (Temp 3)
4. Channel 4 Brightness Temperature (Temp 4)
5. Channel 5 Brightness Temperature (Temp 5)
6. Temp 3 minus Temp 4 (T3-T4)
7. Temp 4 minus Temp 5 (T4-T5)

From this point forward, the parameters will be referred to by their abbreviations in parenthesis.

Cal 2 provides an indication of the solar reflectance of image features. S12L is used to determine smoke distributions over water. It uses the differing absorption characteristic of the Gulf water between channels 1 and 2 to contrast with the smoke signature. Temp 3, during the daytime, contains both reflected solar energy and emitted IR. Temp 4 wavelength band is in a water vapor window and

therefore gives a relatively accurate indication of feature temperatures. Temp 5 also gives feature brightness temperature. Its wavelength band, however, is located just on the edge of the water vapor window so there is some sensitivity to water vapor in the feature brightness temperatures. T3-T4 gives a first order estimate of the reflected solar radiation in Temp 3. T4-T5 has been typically used to sense water vapor effects on sea surface temperature measurements. In this project, however, it is used to separate the dust from other features based on the differing dust absorption characteristic between channels 4 and 5 as previously discussed in Chapter II.

b. Scatter Plot Technique

In the production of a full image, two dimensional scatter plot is a multi-step process. Figure 7 outlines the steps in the procedure. First, two satellite subimages or parameters are selected. Subimages are 512 by 512 picture element (pixel) areas derived from larger overview regions of a satellite pass. The data for each pixel in the subimages is stored in ascii format and must be converted to real numbers. This is done by a Fortran program called "Image to Real". The program converts the ascii data for an image into a 512 by 512 real number array data file. Once the conversion is complete, both arrays are input into a Fortran program called "Get

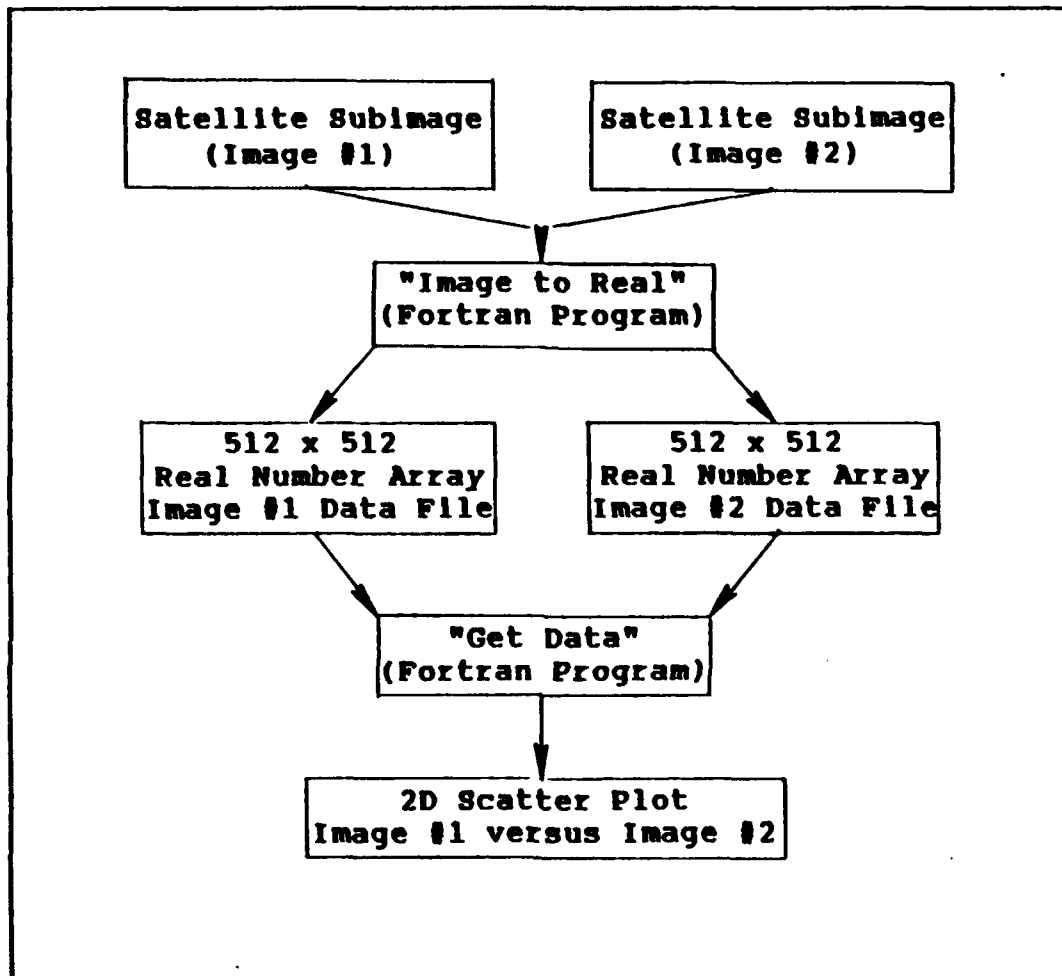


Figure 7. Procedural flow chart for producing full image 2D scatter plot for two subimages.

Data", which plots image one versus image two on a 2D scatter plot. Note, the number of pixels plotted from each image can be varied. Figure 8 is an example of a full image 2D scatter plot with every other pixel plotted.

The next procedure, after producing a full image 2D scatter plot, is to identify the individual feature radiative signatures on the plot. The flow chart (Figure 9) outlines this process. Utilizing a Fortran program called "Store", individual feature areas (e.g., areas of only land, smoke, dust, etc.) can be sampled from a subimage. "Store" then puts the ascii information from the area into a data file. That process is repeated until enough areas are sampled to accurately identify the features of interest on the full 2D scatter plot. Once the desired sample area ascii data files are created for each subimage (keeping the sample area locations consistent for each) individual sample area scatter plots are produced. Figure 10 is an example of a sample area scatter plot. This is done by inputting the individual sample data files into the Fortran program "Get Ascii". "Get Ascii" produces the same scatter plots as "Get Data" except it plots only the sample areas from each subimage versus each other. By doing this, the general location and approximate 2D radiative signature of a desired feature can be analyzed on the full image scatter plot. Each sample area is approximately represented by either an oval or a hand drawn

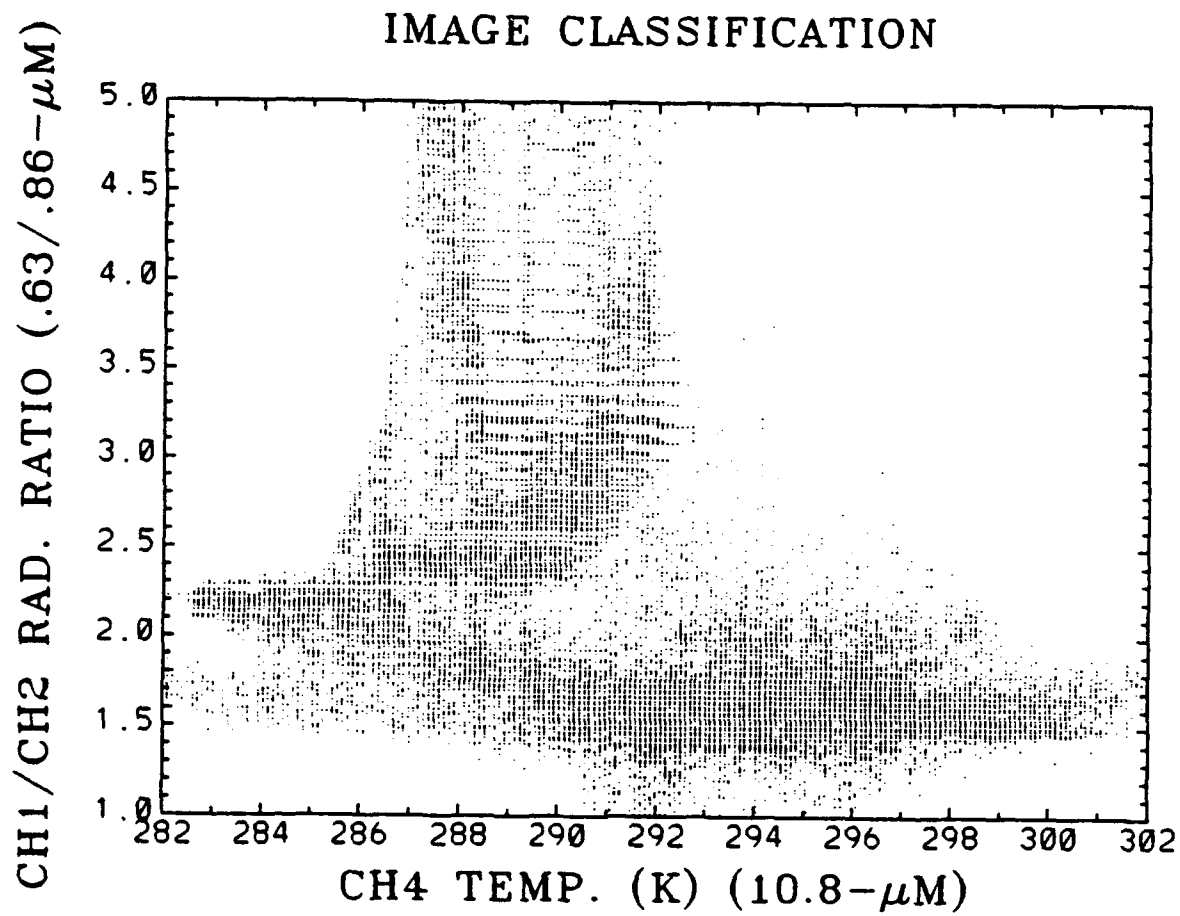


Figure 8. Example of full image 2D scatter plot of S12L versus Temp 4 for area 1 in Figure 14.

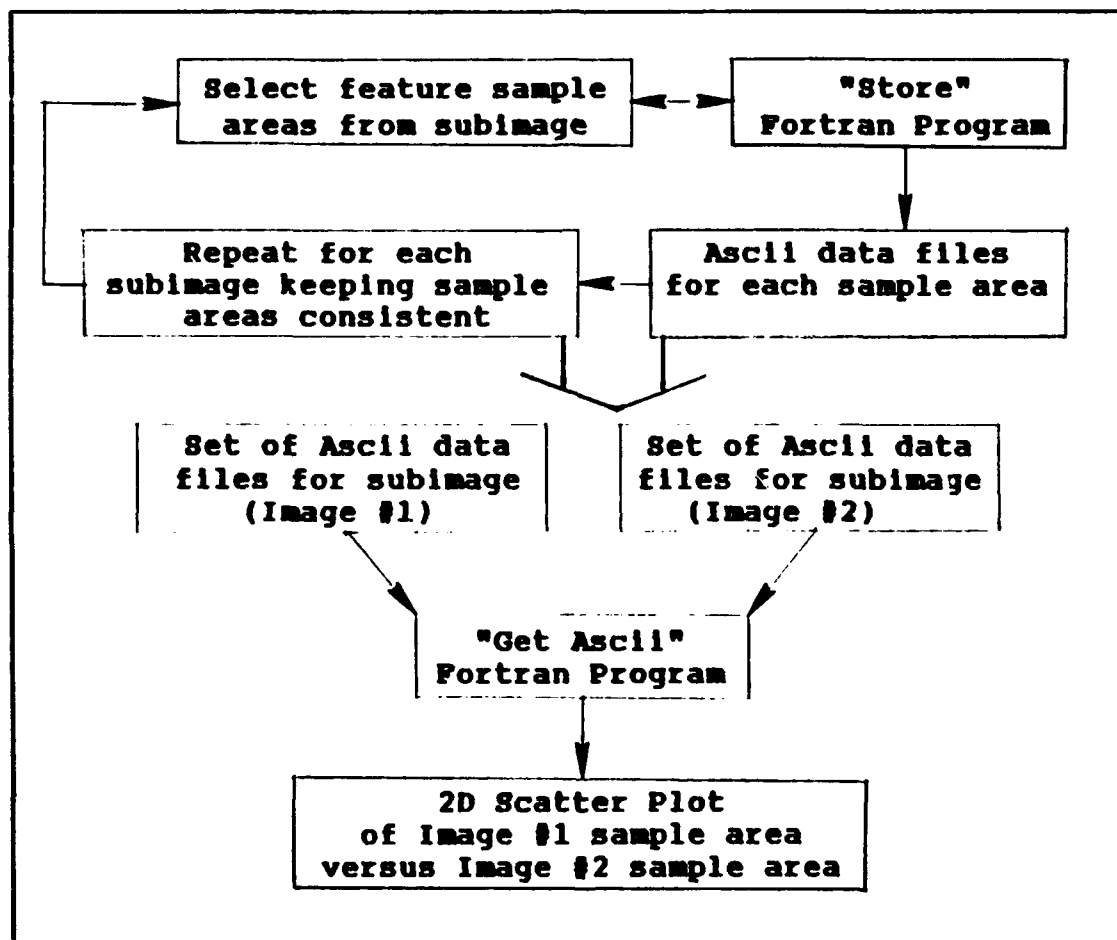


Figure 9. Procedural flow chart for producing image sample areas on 2D scatter plot.

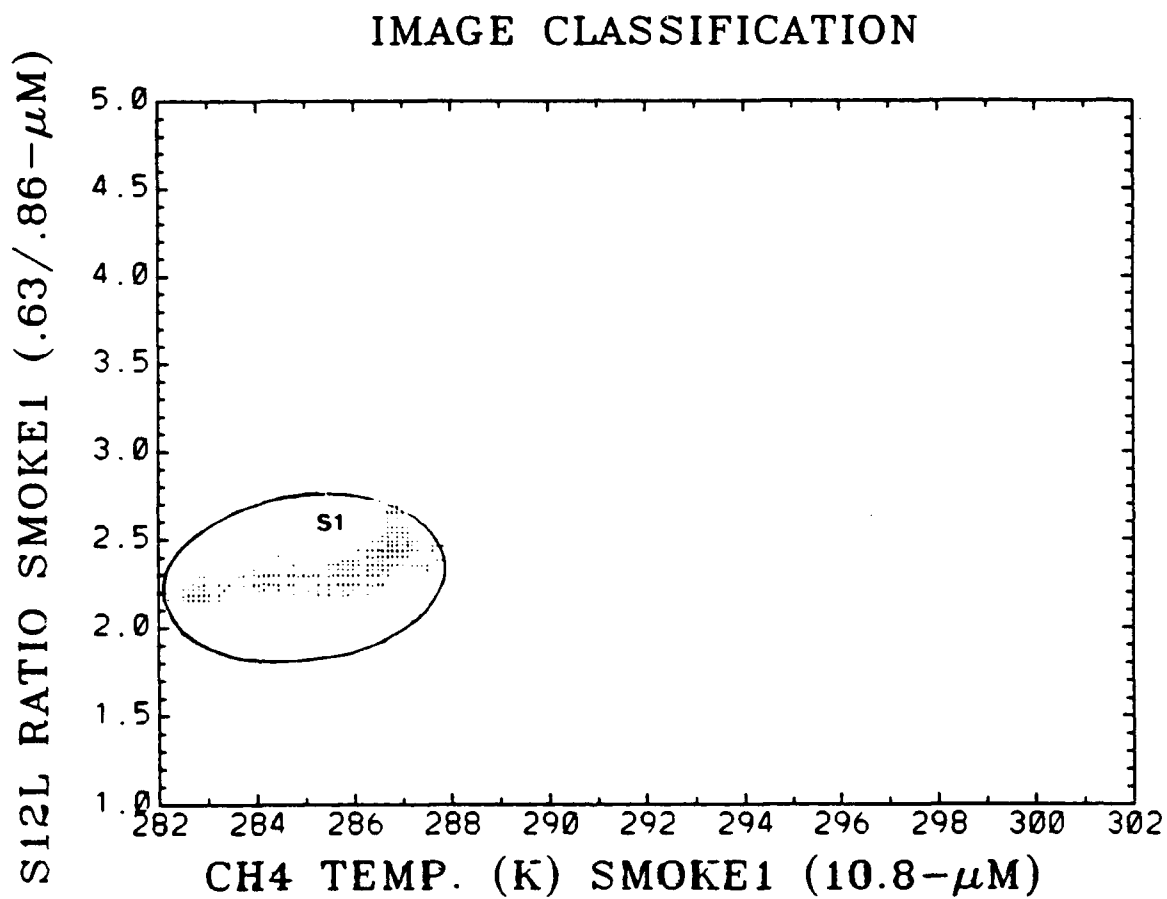


Figure 10. Example of single feature 2D scatter plot. Smoke 1 corresponds to S1 sample area on Upper Gulf images, see Figure 16.

sketch on the full image 2D scatter plot. The goal is to encompass at least 80 percent of the pixels defining a sample area. A hand drawn sketch is used when either the shape of the pixel area representing a feature is not conducive to an oval and/or if 80 percent of the feature cannot be encompassed without highly exaggerating the pixel area defining the feature. The drawing of the ovals and/or hand sketches is subjective and in most cases will not exactly align with the actual analyzed signature limits of the features. They are drawn to give an idea how the feature signatures breakout on the full image scatter plot.

c. Verification of Radiative Signature Analyses

To verify the signatures analyzed using the scatter plot technique, a two dimensional mask program called "Maskit" is utilized. Figure 11 is a procedural flow chart showing this process. Essentially, the analyzed two dimensional limits of a feature are input into "Maskit". The program then colors or masks any pixels falling in the limits with one of seven primary colors. The masked area provides the feedback to validate the analyzed results. Figure 12 is an example of analyzed limits on a scatter plot and Figure 13 is the mask of those limits.

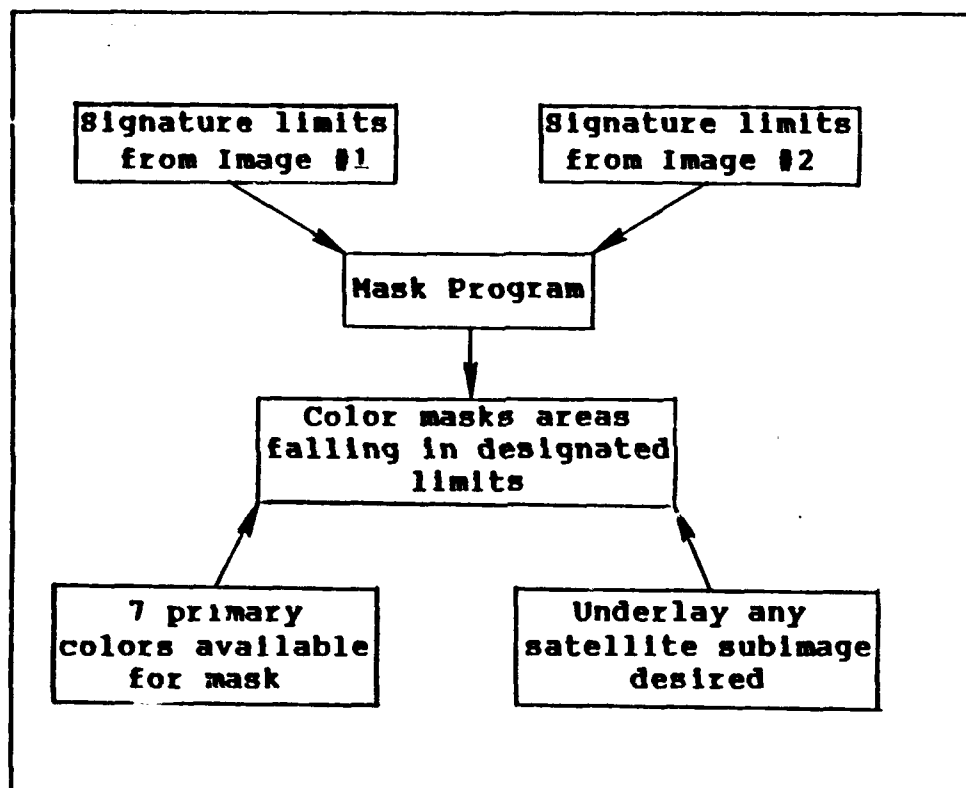


Figure 11. Procedural flow chart for verification of radiative signature analyses.

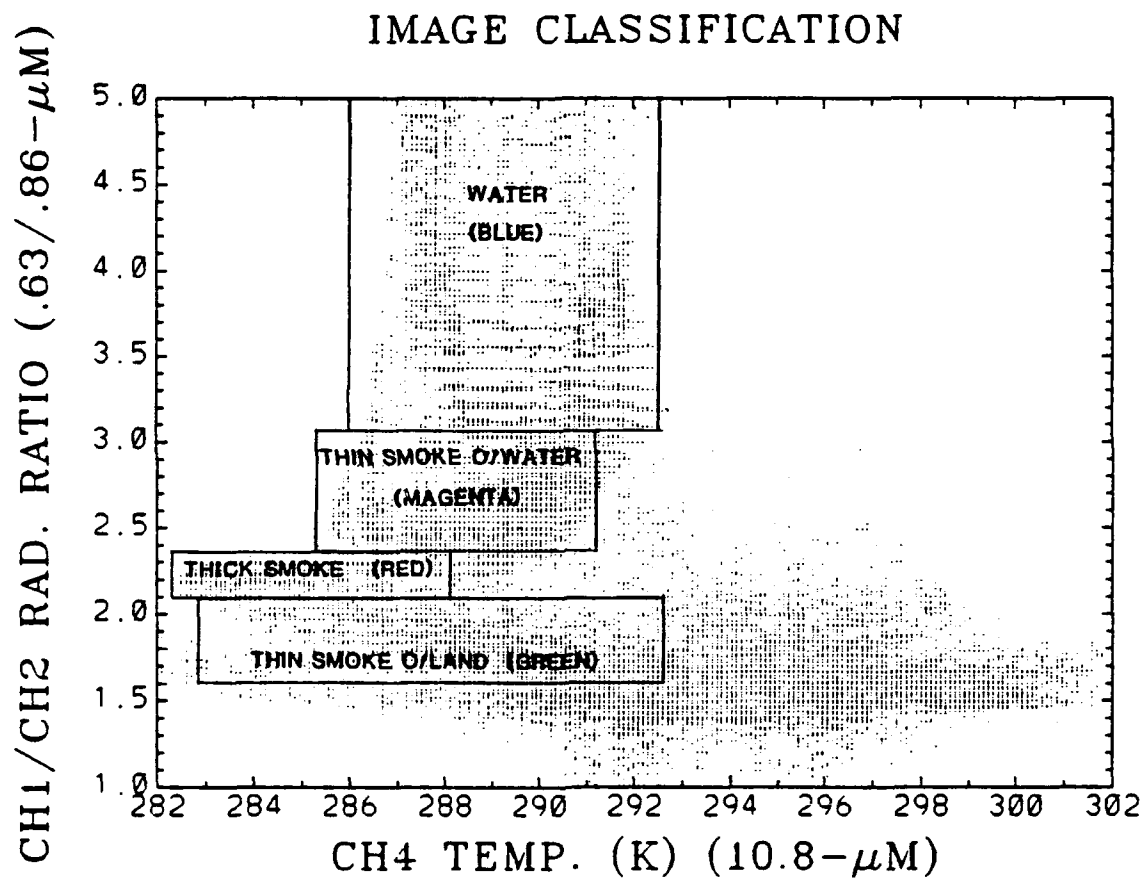


Figure 12. Same as Figure 8 except example of analyzed 2D signature limits on full image 2D scatter plot of S12L and Temp 4 for area 1 in Figure 14. Region represented in this image corresponds with area 1 of Figure 13.

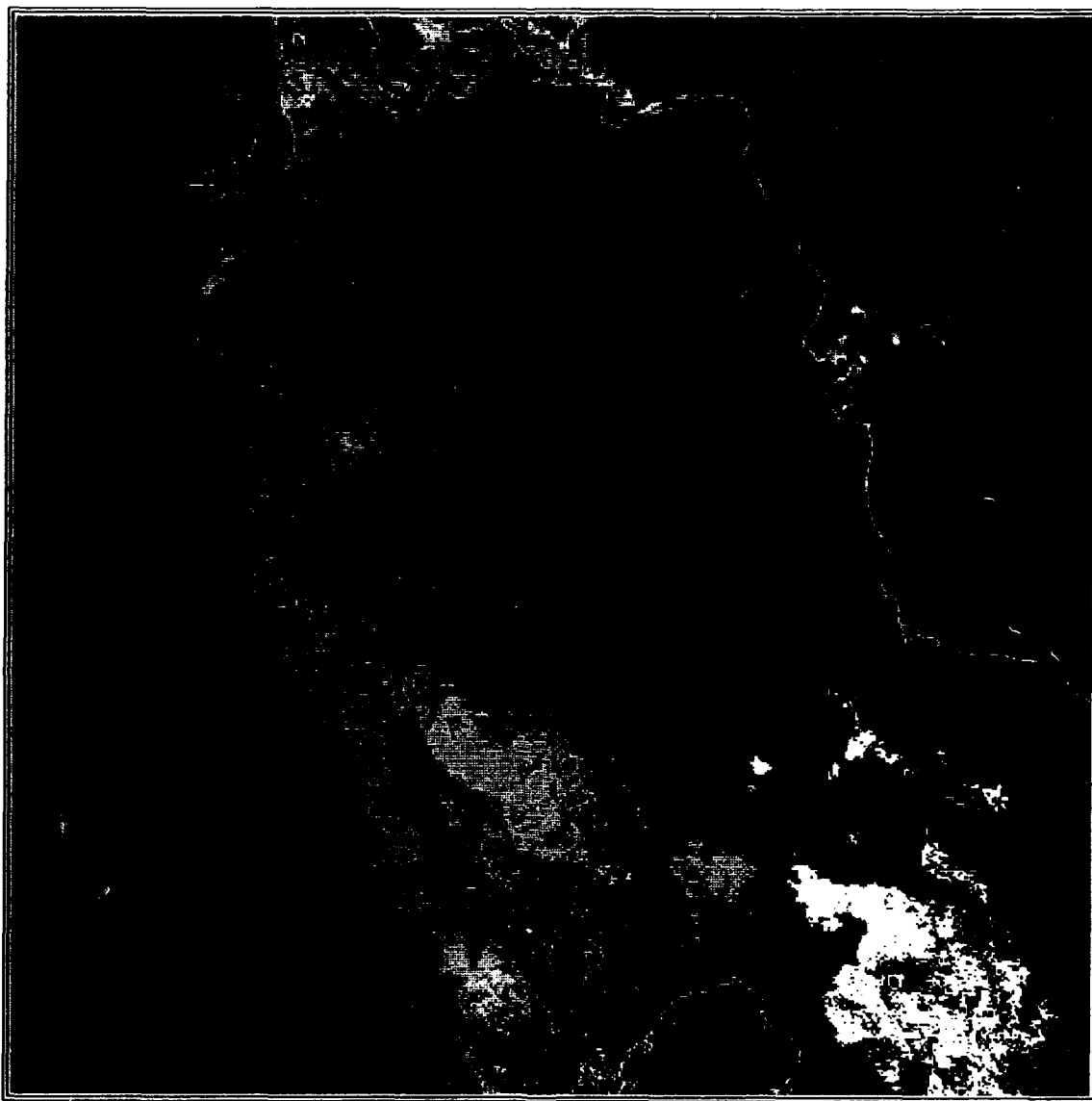


Figure 13. Example of mask using analyzed limits from Figure 12. Red is thick smoke. Green is thin smoke over land. Magenta is thin smoke over water. Blue is water.

IV. SCATTER PLOT ANALYSES/RESULTS

A. UPPER GULF SCATTER PLOTS

The images, used to produce the scatterplots for analysis, cover the same area 1 of the upper Arabian Gulf (see boxed area on map Figure 14). Each image is 512 by 512 picture elements (pixels) in size with a 1.1km per pixel resolution. The images were generated from a NOAA 11 AVHRR Middle East pass taken at 1026 UTC 1 March 1991. The actual scatter plots, although taken from the 512 by 512 images, were generated by sampling every other pixel. Thus the scatter plots effectively have a 2km resolution. Sampling every pixel proved to be too cumbersome and made it generally more difficult to discern the desired signatures.

The following features were analyzed on each scatter plot to determine their radiative signature: 1) water, 2) thick smoke, 3) thin smoke over land, 4) thin smoke over water and 5) land. The "water" signature represents the portions of the gulf without a discernible smoke or cloud overcast. Those areas of "clear" water are primarily concentrated in the far northern gulf and along the Iranian coast. "Thick smoke" refers to smoke with a radiative signature the same as smoke within approximately 10 to 100km of the main oil well fires. As might be expected, the thick smoke areas stretch from the

sources down the central portions of the various plumes. The "thin smoke over land" signature is representative of the land areas just perceptible through the smoke overcast. Those areas are concentrated on the fringes of the smoke plumes. The signature for "thin smoke over water" depicts any water area with a "thin" smoke overcast. The thin smoke over water primarily extends from the plume fringes in the northwest Arabian Gulf through the central gulf down to the southeast where the signature is lost due to dispersion. "Land" with no smoke or cloud overcast accounts for most of the radiative signature indicated on the scatter plots. As will be noted in the following analyses there are essentially four discernible land signatures. Figure 15 presents AVHRR channel 1 to channel 2 radiance ratio image (S12L) of the upper gulf and depicts, with colored boxes, the sampled pixel areas of the features previously listed and described. The S12L and Temp 4 (Figure 16) images served as the "baseline" images to determine feature sample areas. Note some features were sampled in more than one location. As a reminder, on all scatter plots, ovals and/or hand drawn sketches encompass the majority of those pixels which are representative of a particular feature. They are not meant to represent the exact analyzed signature limits. Finally, there was experimentation with a number of image combinations. Only the most illuminating cases, however, are presented.

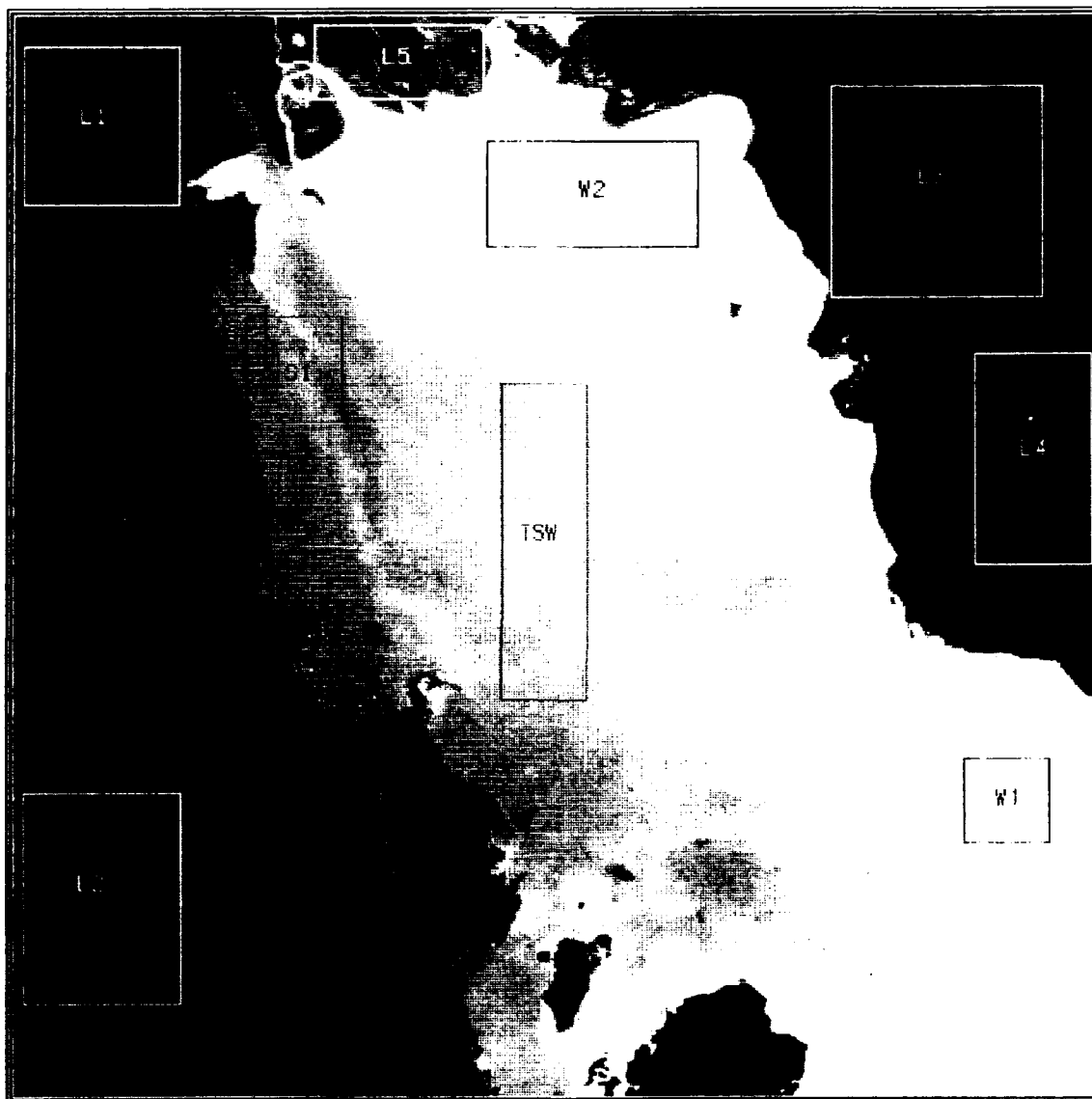


Figure 15. 1 March 1991 1026 UTC Upper Gulf S12L image depicting feature sample areas (L-land, S-smoke, W-water, TSW-thin smoke over water and TSL-thin smoke over land).

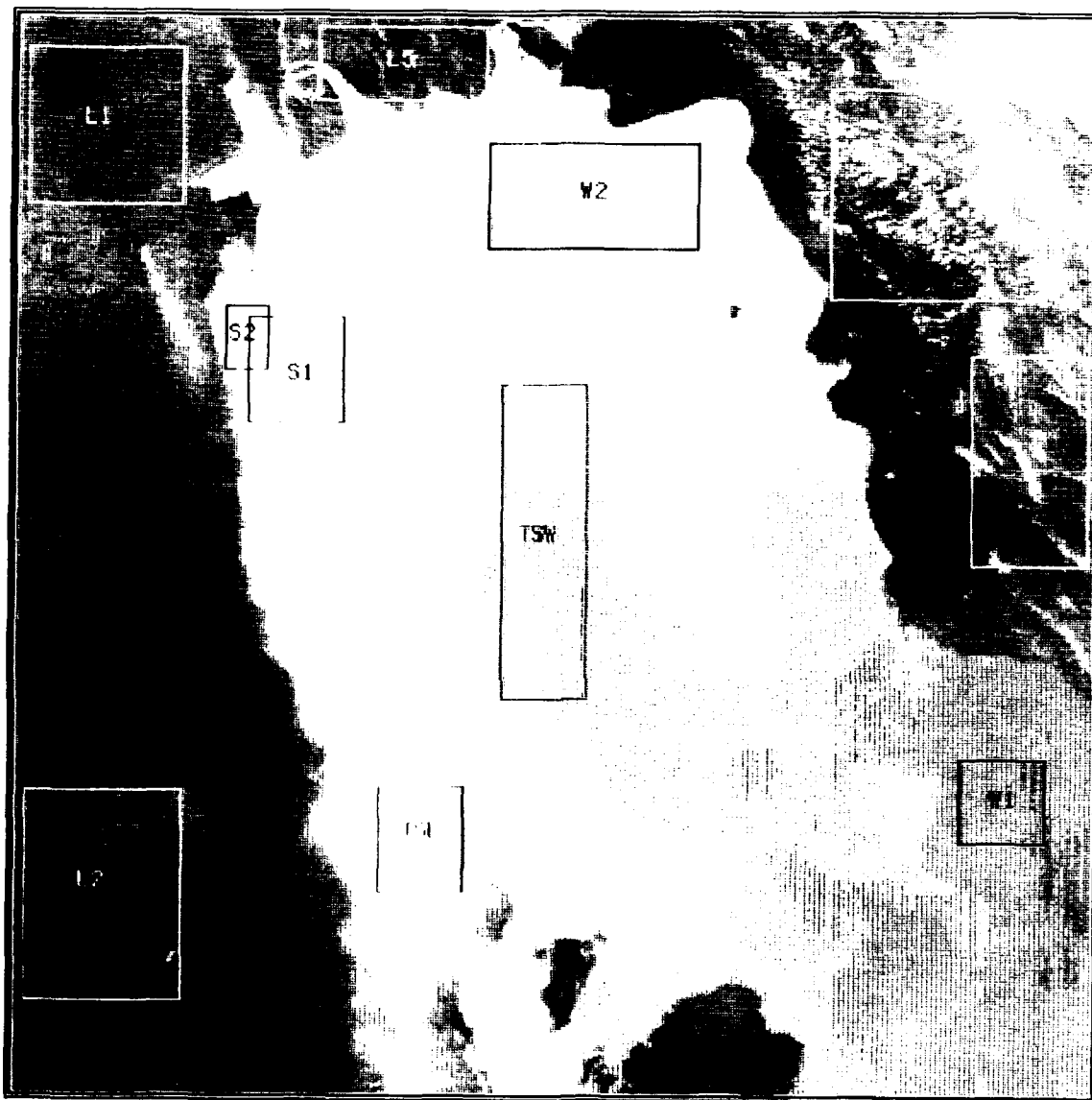


Figure 16. 1 March 1991 1026 UTC AVHRR Temp 4 satellite image used as baseline to select feature sample areas. Areas labelled as in Figure 15.

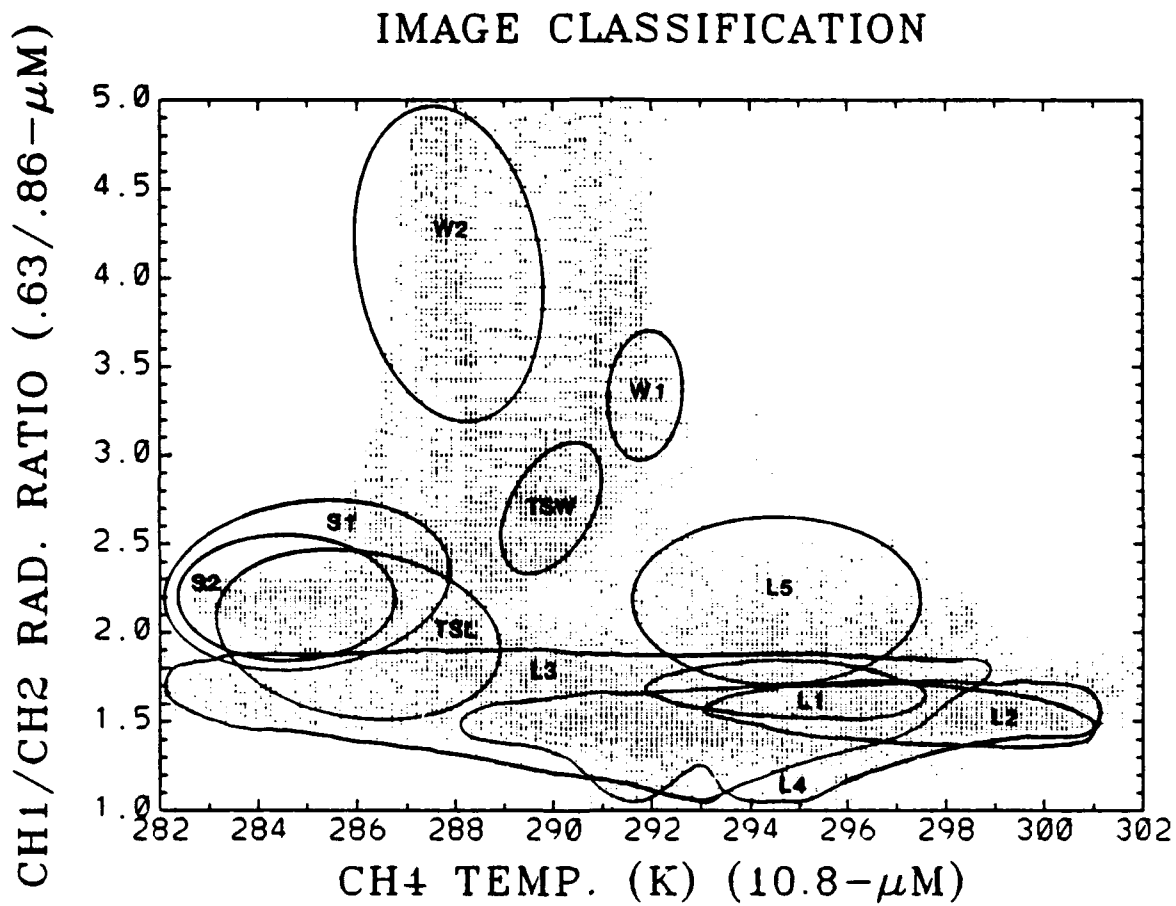


Figure 17. Case 1 Upper Gulf scatter plot. Enclosed areas in Figures 15 and 16 (W-water, L-land, S-smoke, TSW-thin smoke over water and TSL-thin smoke over land).

1. Case 1 Scatter Plot Analysis: S12L Versus Temp 4
(Figure 17)

a. Water:

Water ranges from approximately 3.06 to 5.0 on the S12L axis and from 287.29°K to 292.5°K on the channel 4 temperature axis. "Water" on the S12L image constitutes the brightest feature (mid gray to white). This implies the gulf water reflects more radiation in channel 1 than in channel 2. At this time it should be noted, theoretically given "pure" water with a relatively deep depth (>~10m) the S12L ratio would be close to one. This results from the high absorption for both channels 1 and 2 wavelength bands and because reflectance is low and approximately the same. There are two major factors which account for the differences in reflectance and thus give a relatively high range of radiance ratios. First is the amount of sediment in the water. February and March are climatologically in the middle of the rainy season for the Middle East as indicated (Taha et al., 1981). Consequently, it is assumed there is sediment laden river runoff, primarily in the northern gulf around the Euphrates and Tigris River deltas and in the northwestern gulf, along the coast of Iran, due to various rivers flowing down from the Zagros Mountains. The large amount of sediment in those coastal waters increases the reflectance of the water in both

channels 1 and 2. But because channel 2 has a wavelength band at the end of the visible spectrum and into near IR, the water absorbs more at those wavelengths compared to channel 1, which has a wavelength band wholly in the visible spectrum. In fact, channel 1 wavelengths are absorbed approximately 5 times less than those of channel 2.

The second factor accounting for the radiance variation between channels 1 and 2 is the bathymetry of the gulf. Although the variation is not as dramatic as that attributed to the sediment, there is a correlation between water depth and the magnitude of the S12L ratio. As the water depth increases the radiance ratio decreases. Especially evident of this correlation is the outline of the 10 fathom line on the S12L image. The explanation for this correlation appears to be twofold. First, near surface suspended sediment correlation decreases as a function of distance from shore due to particle settling and dispersion. Since the amount of suspended sediment seemingly drives the amount of channel 2 waveband absorption (i.e., the more sediment the more absorption) it makes sense that channel 2 and channel 1 radiances would get closer, meaning the magnitude of the S12L ratio would decrease - as it does. Second, with increasing water depth, there is increased absorption in both channels. In other words, once a photon from either waveband enters the water, the deeper the water the less chance the photon has to be scattered back out. Therefore, as water depth increases,

the observed radiances in channels 1 and 2 decrease and begin to equalize. This translates to lower and lower S12L ratios or darker and darker gray shades on the S12L image. The channel 4 temp range for water, as indicated earlier, is approximately 286°K to 292.5°K. As might be expected the cooler water is in the northern gulf and warmer water in the South. Latitudinal air temperature variations as well as the influx of cool river water in the northern gulf are suspected as the primary reasons for the 6.5°K temperature difference.

b. Thick Smoke:

Thick smoke ranges from approximately 2.10 to 2.37 on the S12L axis and from 282.2°K to 288.11°K on the channel 4 temperature axis. The S12L ratio of around "2" implies the smoke particles are approximately twice as reflective of the channel 1 wavelength band compared to channel 2's. That, however, is most likely not the case. Due to intrusion of water into the oil wells, water vapor, in addition to smoke particles and a myriad of other gases, became a combustion product (Limaye et al., 1991). As a result, the smoke particles act as condensation nuclei and introduce liquid water into the smoke plume. Since water is slightly more absorptive of channel 2 wavelengths, observed channel 1 radiance is slightly higher which accounts for an S12L ratio greater than 1.

The channel 4 thick smoke temperatures should be very representative of the actual temperatures at the top of the smoke layer. USS Wisconsin (BB 64) (1991), post cruise report indicates total obscuring of the sun near the source(s) which likely translates to very little IR contamination/contribution to the observed smoke top temperature due to surface/ground emittance.

c. Thin Smoke Over Land:

Thin smoke over land ranges from approximately 1.61 to 2.09 on the S12L axis and from 282.6°K to 292.59°K on the channel 4 temperature axis. The lower S12L ratios (compared to thick smoke) are primarily due to the surface/ground reflectance contribution to the thin smoke signature. The observed surface/ground radiances are approximately the same in channels 1 and 2 which implies an S12L ratio of around 1. Thus, the "ground contamination" decreases the thin smoke ratio.

Surface/ground IR emittance also accounts for the slightly higher channel 4 temperature range for the thin smoke. Compared to totally obscured, as near the sources, the ground receives some solar radiation and is heated slightly. The heating results in surface IR emittance and a larger temperature range for the thin smoke over land.

d. Thin Smoke Over Water:

Thin smoke over water ranges from approximately 2.38 to 3.05 on the S12L axis and from 285.25°K to 291.17°K on the channel 4 temperature axis. The signature for thin smoke over water is strongly influenced by the water over which it lies. As in the case of thin smoke over land the water radiance contaminates the basic smoke signature and this accounts for the higher S12L ratio and warmer temperature 4 range - as compared to thick smoke.

e. Land:

Land primarily ranges from 1.0 to slightly above 2.5 on the S12L axis and is spread across the full range of channel 4 temperatures with most of the signature concentrated above 290°K. The reason for the diversity in signature rests in the fact there are essentially four different land features in the images. The features vary from desert, irrigated/vegetated plots, river deltas and finally snow covered mountainous areas. In general, however, the land areas are the warmest features in channel 4 temp and the darkest (lowest ratio) in S12L. The warm signature occurs because the satellite data was taken at 1426 local time - the land should be close to its warmest diurnal temperature. The relatively small range in S12L implies most land features have the same reflectance in channel 1 as in channel 2.

f. Summary:

The S12L versus channel 4 temp scatter plot highlights the signatures of the five main features quite well. Water is confined to a relatively narrow low to mid axis temperature range of 6.5°K but accounts for the highest S12L ratios. This translates to water appearing as a light gray on the temperature 4 image and mid level gray to white on the S12L image. Thick smoke lies at the low end of the temperature axis and covers about a 6°K temperature span. Its S12L image is very narrow ($\sim .3$) and is centered around a ratio of 2.23. Thick smoke appears as a very light to almost white gray shade on the temperature 4 image and as dark gray on the S12L image. Thin smoke over land has a temperature signal spread across the lower half of the temperature 4 axis but has a relatively narrow ($\sim .5$) S12L range centered at 1.85. Its overall signature is driven by the land it covers, which accounts for the wide temperature range and narrow S12L ratio. It appears across the full spectrum of mid-level grays in the temperature 4 image and as a dark gray (not black) on the S12L image. Thin smoke over water covers a 6°K , low to mid, temperature range and lies in a .7 S12L ratio range centered at approximately 2.73. As with its counterpart over land, the water has a significant influence on its signature. Thin smoke over water appears as a light gray on the temperature 4 image (almost indiscernible from the water) and as a mid level dark gray on the S12L image. The highly variable land

signature is also the most dominant feature on the scatter plot. It lies across the entire temperature axis and accounts for the lowest S12L ratios. It appears anywhere from the darkest gray (black is the actual oil fires) to white on the temp 4 image and from black to dark gray on the S12L image.

Overall, this scatter plot separates the signatures of the five main features the best. Its most important aspect, however, is the separation of thin smoke over water. Even though the range limits are highly subjective, this is the only plot that discernibly separates the thin smoke over water from the other features.

2. Case 2 Scatter Plot Analysis: Cal 2 Versus Temp 4 (Figure 18)

a. Water:

Water ranges from approximately .7 to 1.7 percent albedo on the channel 2 axis and from 287.29°K to 292.5°K on the channel 4 axis. The channel 4 temperature range was previously discussed in case 1. The channel 2 albedo range confirms what is generally known about water - that it has a low albedo especially when the sun is close to its zenith, as in this case (Kidder and Vonder Haar, 1992). Therefore, water appears black in the channel 2 image.

IMAGE CLASSIFICATION

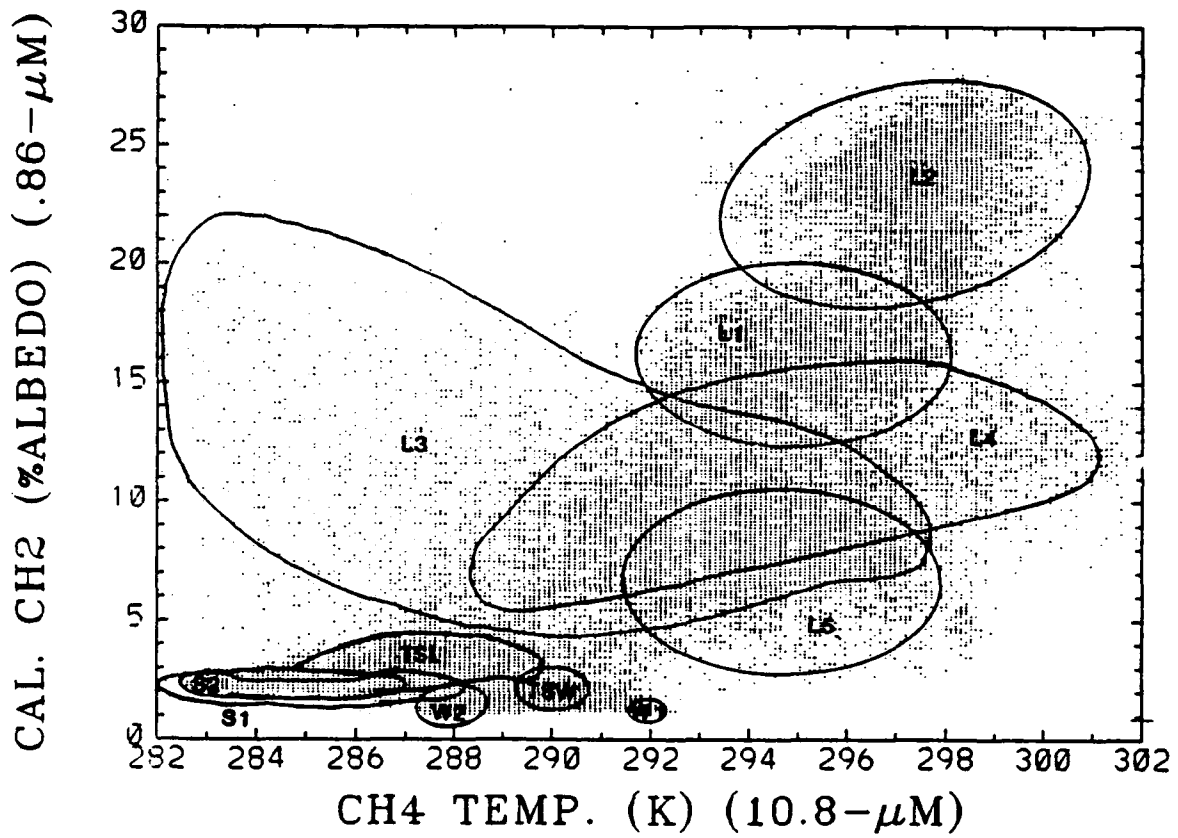


Figure 18. Case 2 Upper Gulf scatter plot. Feature designation as in Figure 17.

b. Thick Smoke:

Thick smoke ranges from approximately 1.7 to 2.9 percent albedo on the channel 2 axis and from 282.3°K to 288.11°K on the channel 4 axis. The channel 4 range is consistent with that analyzed in case 1. The low albedo of smoke in channel 2 implies the smoke particles are highly absorbent of incident solar radiation. In fact, almost no visible light is reflected from the particles. The light that is reflected is most likely a result of scattering by the condensed water on the larger smoke particles.

c. Thin Smoke Over Land:

Thin smoke over land ranges from approximately 2.0 to 4.0 percent albedo on the channel 2 axis and from 282.9°K to 287.8°K on the channel 4 axis. The albedo signature is higher than the thick smoke albedo because the particle density is less which allows visible light reflected from the primarily sand surface to boost the albedo slightly. The temperature range is consistent with that analyzed in case 1.

d. Thin Smoke Over Water:

Thin smoke over water signature ranges from approximately 1.4 to 2.1 percent albedo on the channel 2 axis and from 285.25°K to 291°K on the channel 4 axis. Note, these ranges are the most subjective of all the features. Because of the low albedo of both smoke and water it is extremely difficult to discern a cutoff. Considering the resolution of

the images and scatter plots, the cutoff is probably indiscernible. Overall, however, the albedo signature is generally lower than both the thick smoke and thin smoke over land signatures. This is due to the influence of the very low water albedo. The temperature 4 signature is consistent with that analyzed in case 1.

e. Land:

The land signature ranges from approximately 2.0 to 30.0 percent albedo on the channel 2 axis and covers the full temperature range on the channel 4 axis. There were some pixels higher than 30 percent albedo but the channel 2 axis was limited to 30 to enhance the "main" image features. Those pixels higher than 30 percent albedo constitute areas of highly reflective snow, in the Zagros mountains (upper right corner of image, Figure 19), and some small patches of desert sand on the west coast of the gulf (lower left corner of image Figure 19). The lower albedos represent the vegetated/irrigated areas. Once again, the temperature 4 signature is consistent with that analyzed in case 1.

f. Summary:

Overall, the scatter plot indicates smoke and water have similar albedo characteristics. Water, thick smoke and thin smoke over water/land are concentrated between .7 to 4.0 percent albedo. This translates to very little separation. Water is at the low end of the albedo range and thin smoke



Figure 19. 1 March 1991 1026 UTC Upper Gulf Cal 2 image. Brightness pixels in upper right and lower left corners are areas with an albedo greater than 30 percent.

over land is at the high end. The temperature differences of the features account for most of the small signature separation observed. The "standout" signature on this plot is that of the land. In fact, there is excellent separation of the individual land regions. This separation especially emphasizes the diversity of land in the upper gulf region.

3. Case 3 Scatter Plot Analysis: T3-T4 Versus Temp 4 (Figure 20)

In channel 3 there is contribution to total daytime radiance from both the solar and thermal IR spectrums. Thus, channel 3 daytime brightness temperatures do not represent just thermal emission but are "contaminated" with some reflected solar radiance. For this reason, observed channel 3 daytime brightness temperatures are generally higher than those observed in a strictly thermal IR channel such as channel 4. Therefore, when a channel 3-4 temperature difference image is produced most values are positive as can be seen on the scatter plot.

a. Water:

Water ranges from approximately -0.8°K to 4.0°K on the T3-T4 axis and from 287.29°K to 292.5°K on the channel 4 temperature axis. It has the lowest difference range of the main features. This is consistent with the low albedo of water. Because water does not reflect much solar radiation

IMAGE CLASSIFICATION

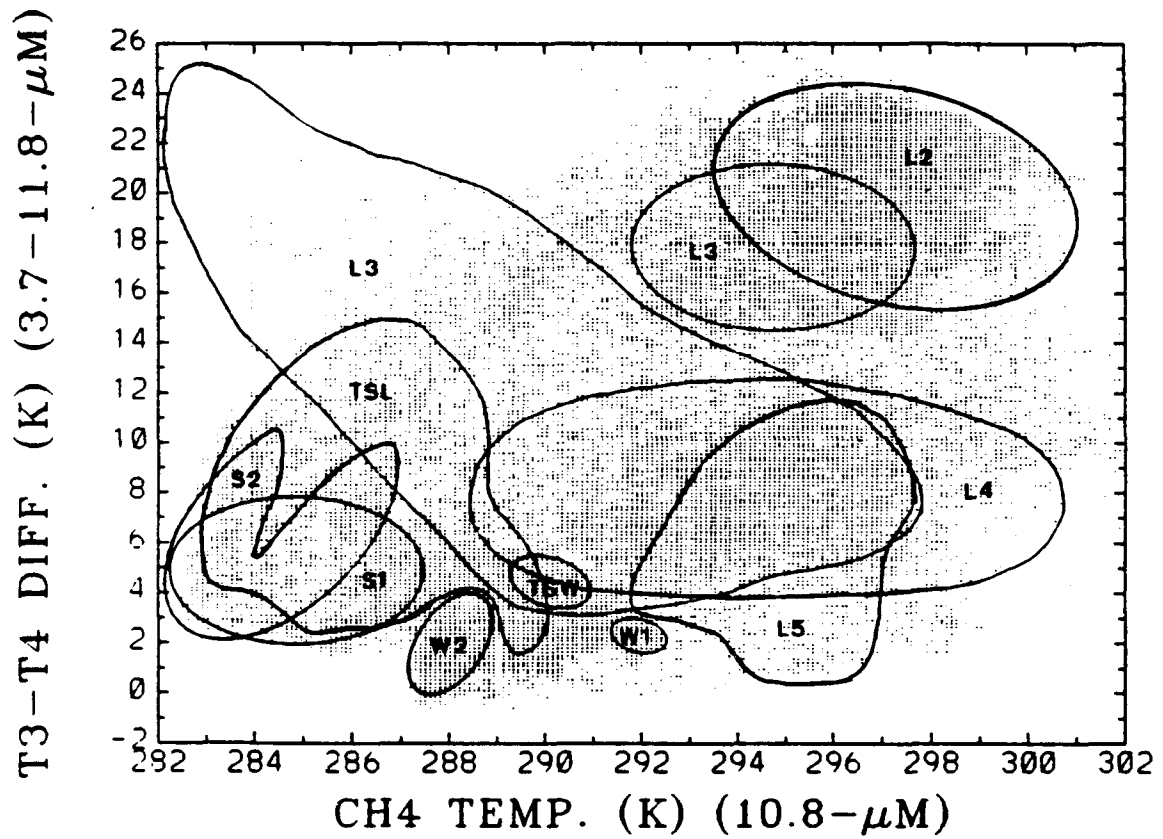


Figure 20. Case 3 Upper Gulf scatter plot. Feature designation as in Figure 17.

its brightness temperature in channel 3 are close to those in channel 4. The upper limit is most likely indicative of the shallower, sediment laden water and the lower limit indicative of the deeper, reduced sediment water due to the differences in reflectance as discussed in case 1. The channel 4 temperature range is consistent with those analyzed cases 1 and 2. The temperature bounds, however, were more definitive in this scatter plot and thus easier to analyze.

b. Thick Smoke:

Thick smoke ranges from approximately 2.2°K to 9.0°K on the T3-T4 axis and from 282.2°K to 288.11°K on the channel 4 axis. The bottom limit on T3-T4 axis is relatively discrete but the upper limit is highly subjective which emphasizes the complexity of the thick smoke areas. Due to the reflective component in channel 3, the thick smoke signature is dispersed over a wide range of T3-T4 values.

The thick smoke sample areas (see S1 and S2 boxes on Figure 21) encompasses smoke over both land and water and part of the "fringe" areas of the smoke plumes. The land (sand) in that area has a relatively high albedo. That reflective influence in the fringe areas furthest from the fires, is what drives the channel 3 temperature higher and is responsible for the higher T3-T4 values at the warmer channel 4 temperatures (286°K - 287°K range). The higher T3-T4 values

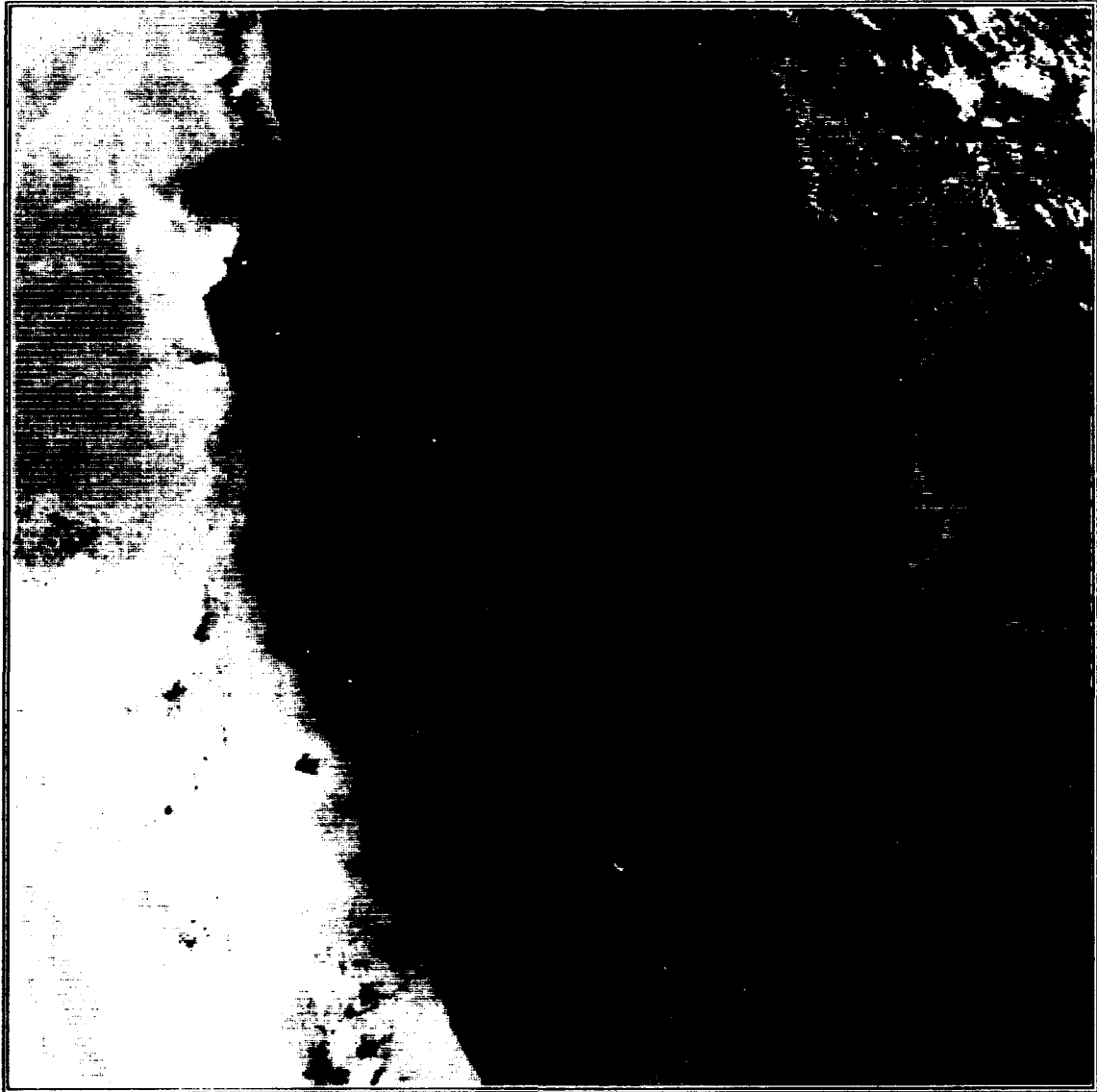


Figure 21. 1 March 1991 1026 UTC T3 T4 Upper Gulf image. S1 and S2 boxes encompass smoke over both land and water.

in the cooler channel 4 temperature range (283°K - 284°K) are probably driven in a small part by the land reflectivity but in a large part due to the back scattered visible radiation by the water drops attached to the smoke (this is in the area nearest the fires where the atmospheric water vapor content is the highest). Note this is purely speculation to account for the two "thick smoke branches" seen on the scatter plot. The thick smoke values in the 3.8°K to 5.6°K range on the T3-T4 axis can most likely be accounted for by the varying amounts (albeit small) of added reflectance in channel 3 from the gulf water.

The lowest T3-T4 values represent the thickest smoke. The denser and thicker the smoke, the less chance there is for reflective influence in channel 3 from the land or water which implies the 3-4 temperature difference should be low. The thickest smoke channel 4 temperature spread is primarily due to whether the smoke lies over land (cooler temps) or water (warmer temps). The channel 4 temperature range is consistent with that analyzed in the previous cases.

C. Thin Smoke Over Land:

Thin smoke over land ranges from approximately 2.0°K to 16.0°K on the T3-T4 axis and from 282.9°K to 289.8°K on the channel 4 axis. As with thick smoke, it is dispersed over a wide T3-T4 range. The reason is twofold. First, as discussed under thick smoke, the high albedo of the sand

surface contributes to the anomalously high channel 3 brightness temperatures which cause the positive T3-T4 difference values. Second, the T3-T4 range is large because the contribution by surface reflectiveness is inversely proportional to smoke thickness. The thicker the smoke, the more sunlight is blocked from the surface and the lower the surface reflectance. There is a possibility that some of the lowest T3-T4 values may result not only because of the previous relationship but because there may be a large patch of vegetated land (farmland) under the thin smoke area. These patches would have very low albedos and thus little reflectance contribution to channel 3 brightness temperature. Note, the actual existence of those vegetated areas is unverified. The closeness of these patches to populated areas is the cause for speculation. The channel 4 temperature range is consistent with the previously analyzed cases.

d. Thin Smoke Over Water:

Thin smoke over water ranges from approximately 3.2°K to 6.0°K on the T3-T4 axis and from 285.25°K to 291.17°K on the channel 4 axis. The influence of the slight reflective component of the water is responsible for the larger channel 3 temperature and thus the positive T3-T4 values. The channel 4 temperature limits are consistent with the previous case and as with case 1 and 2 the limits are very subjective.

e. Land:

The land signature ranges from approximately 1.8°K to 26°K on the T3-T4 axis and across the full temperature range on the channel 4 axis. Once again, as in case 2, the diversity of the land features is illustrated quite well. The reflectance of a particular land feature is the key to determining its T3-T4 value. As might be expected, the sand areas and snow covered mountain areas dominate upper part of the T3-T4 axis. Whereas, the river deltas and vegetated areas (like L5) are found at the low end of the T3-T4 range. The channel 4 temperature range is consistent with cases 1 and 2.

f. Summary

The signature separation is indiscrete between thick smoke and thin smoke over land/water. There is, however, fairly definitive separation of those features from the water and land signatures. Water dominates the low T3-T4 values and has a discrete lower channel 4 temperature limit. This is in contrast to the previous two scatter plots (Figures 17 and 18). Understand, however, this lower limit represents gulf water without a smoke overcast. It is expected the water overlain by the smoke has slightly cooler temperatures. The smoke signature, in general, lies to the far left (lower temperatures) on the channel 4 temperature axis but is spread across a large T3-T4 difference range of 14°K. It is difficult to discern a cutoff between thick and thin smoke.

But essentially, the thick smoke is at the lower T3-T4 values and the thin smoke at the higher values. The thin smoke signatures, over land and water, appear to be strongly influenced by surface reflectance. The predominance of the sand surface drives the thin smoke overland signature to the high T3-T4 values whereas the low albedo of the water brings the thin smoke over water signature to the low to mid range values (3-6).

Overall, this scatter plot emphasizes the significance of the reflective component on the brightness temperature in channel 3. The reflectance factor tends to make the brightness temperatures anomalously high; as indicated by most features on the scatter plot having a positive T3-T4 signature. Generally, any feature with a low albedo, such as water or smoke falls toward the low end of the axis and any with a high albedo, such as snow or sand, falls at the upper end. The "standout" signatures as in case 2, are the land features. This scatter plot once again accentuates the diversity of the land in the upper gulf region.

4. Case 4 Scatter Plot Analysis: T3-T4 versus Cal 2 (Figure 22)

As analyzed in case 3, the influence of the reflectance component on channel 3 brightness temperatures is what seems to control the T3-T4 difference values. The idea of this scatter plot is to compare that reflectance component

IMAGE CLASSIFICATION

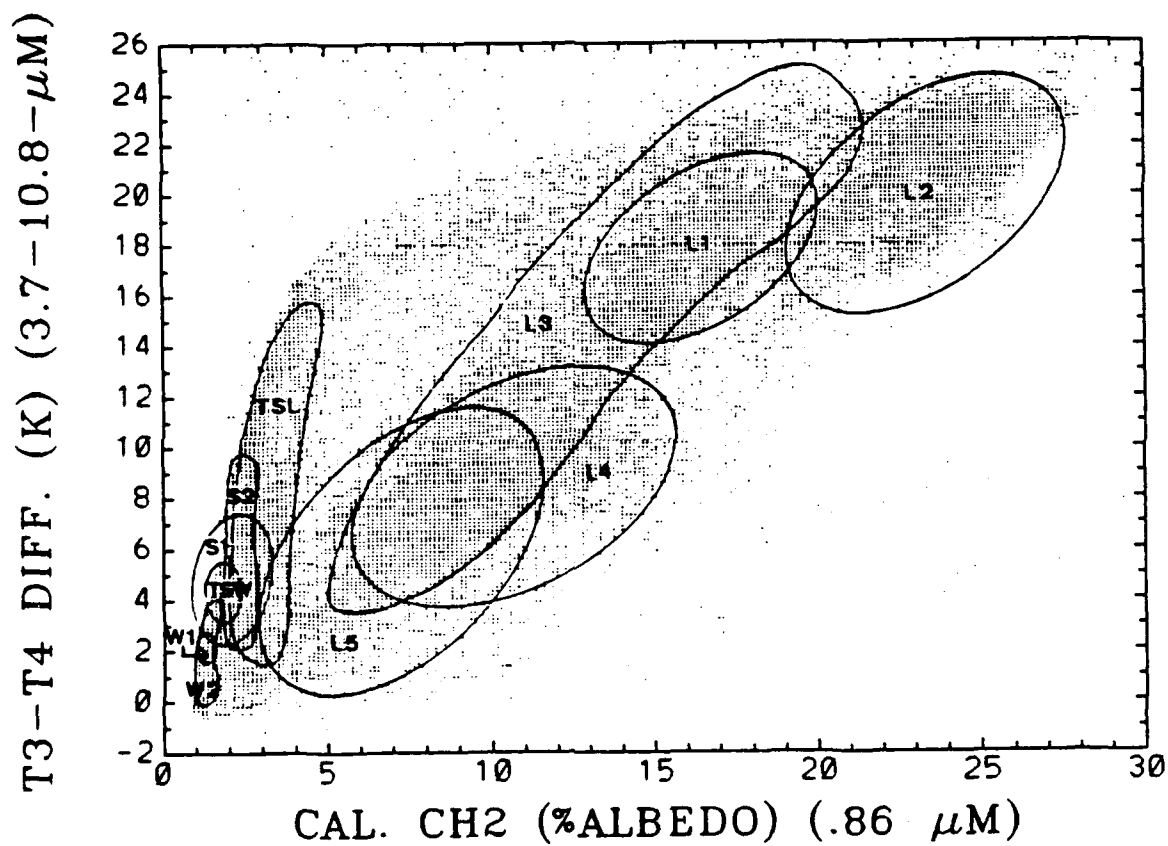


Figure 22. Case 4 Upper Gulf scatter plot. Feature designation as in Figure 17.

against the albedos of the features to draw out the actual contribution reflectance makes towards increasing the channel 3 brightness temperatures for each feature.

a. Water:

Water ranges from approximately -0.8°K to 4.0°K on the T3-T4 axis and from .9 to 1.7 percent albedo on the Cal 2 axis. These ranges are consistent with those analyzed in cases 3 and 2. Water has a low albedo and thus its reflectance does not significantly increase its channel 3 brightness temperature. Therefore, the water signature resides in the lower left corner of the scatter plot at a low T3-T4 difference and a low albedo.

b. Thick Smoke:

Thick smoke ranges from approximately 2.2°K to 9.0°K on the T3-T4 axis and from 1.7 to 2.9 percent albedo, consistent with cases 3 and 2. The relationship here, however, hints the reflectance component is not a major factor in increasing the T3-T4 difference for the smoke. There is some slight dependence, but comparing the ranges shows a 6.8°K T3-T4 difference range compared to a 1 percent albedo range. In other words, as the T3-T4 value goes up, albedo changes very little - there is not a linear relationship. This implies the thick smoke is acting more like a "blackbody" at $3.7\mu\text{m}$ (channel 3) than at $10.8\mu\text{m}$ (channel 4) because it is

emitting more IR radiation at $3.7\mu\text{m}$; which corresponds to the channel 3 brightness temperatures being higher than in channel 4.

c. Thin Smoke Over Land:

Thin smoke over land ranges from approximately 2.0°K to 19.0°K on the T3-T4 axis and from 2.0 to 12.0 percent albedo on the channel 2 axis. The upper limits are not consistent with case 3 and 2. They are more discernible on this scatter plot but are still highly subjective. As with thick smoke, the reflectance component does not appear to be the key to increasing the T3-T4 difference. The reasons for this were discussed under thick smoke. Note, however, the thinner the smoke gets, the more linear the relationship between albedo and the T3-T4 difference (reflectance component). In fact, it becomes almost linear at a T3-T4 difference of 16°K . At that point the reflectance component in channel 3 temperature is the main factor increasing the T3-T4 difference.

d. Thin Smoke Over Water:

Thin smoke over water ranges from approximately 3.2°K to 6.0°K on the T3-T4 axis and from 1.4 to 2.1 on the channel 2 axis, consistent with cases 3 and 2. The signature is being influenced by the low albedo of the water. But once again the characteristic of the smoke particles to radiate more IR in channel 3 than channel 4 is controlling the T3-T4

difference. The signature tends to blend in with the thick smoke signature.

e. Land:

The land signature ranges from 1.8°K to 26°K on the T3-T4 axis and from 2.0 to 30.0 percent albedo on the channel 2 axis, consistent with cases 3 and 2. The land demonstrates, along with its diversity, the most linearity between the T3-T4 difference and albedo. The increasing T3-T4 values appear highly dependent on the reflectance component in channel 3 brightness temperatures. Additionally, the signatures of the individual land areas are well defined.

f. Summary:

The scatter plot has proven to be significant in identifying an important characteristic of the smoke particles. That is, they seem to absorb/emit channel 3 IR wavelengths better than channel 4 wavelengths. This characteristic is what controls the increasing T3-T4 values for the thick smoke and thin smoke over water signatures and the lower T3-T4 range of the thin smoke over land signature. The reflective component in the channel 3 brightness temperature has very little influence on those signatures. Its importance increases, for thin smoke over land, to the point where the smoke has dispersed enough to allow the surface reflectance to become the key factor in boosting the T3-T4 difference. The land and water signatures behave as

might be expected. The water is concentrated at the lower left corner of the scatter plot (low albedo and low T3-T4 value) and the land shows a linear correlation between an increasing albedo and increasing T3-T4 difference.

B. ARABIAN PENINSULA SCATTER PLOTS

The Arabian Peninsula scatter plots were produced from images which are bound by the following latitudes and longitudes: 15° to 27° north latitude by 41° to 53° east longitude (see boxed area on map Figure 14). All images were "remapped" from the NOAA 11 AVHRR Middle East overview taken at 1026 UTC 1 March 1991. They are 512 by 512 pixels in size. But, because they represent a larger area than the Upper Gulf images, they have an approximate 2.5km per pixel resolution vice a 1.1km per pixel resolution.

The following seven main features were sampled on each image: 1) water, 2) clouds, 3) land, 4) dust, 5) high altitude dust, 6) smoke and 7) smoke mixed with and/or overlaying dust. Figure 23 shows where these features were sampled. Note water and land were sampled in three areas each, clouds were sampled in two areas, and smoke, dust, high dust and smoke/dust mixed were sampled in only one area each. The majority of pixels representing each sample area are encompassed on the scatter plots, using ovals and/or hand drawn sketches as in the Upper Gulf cases.

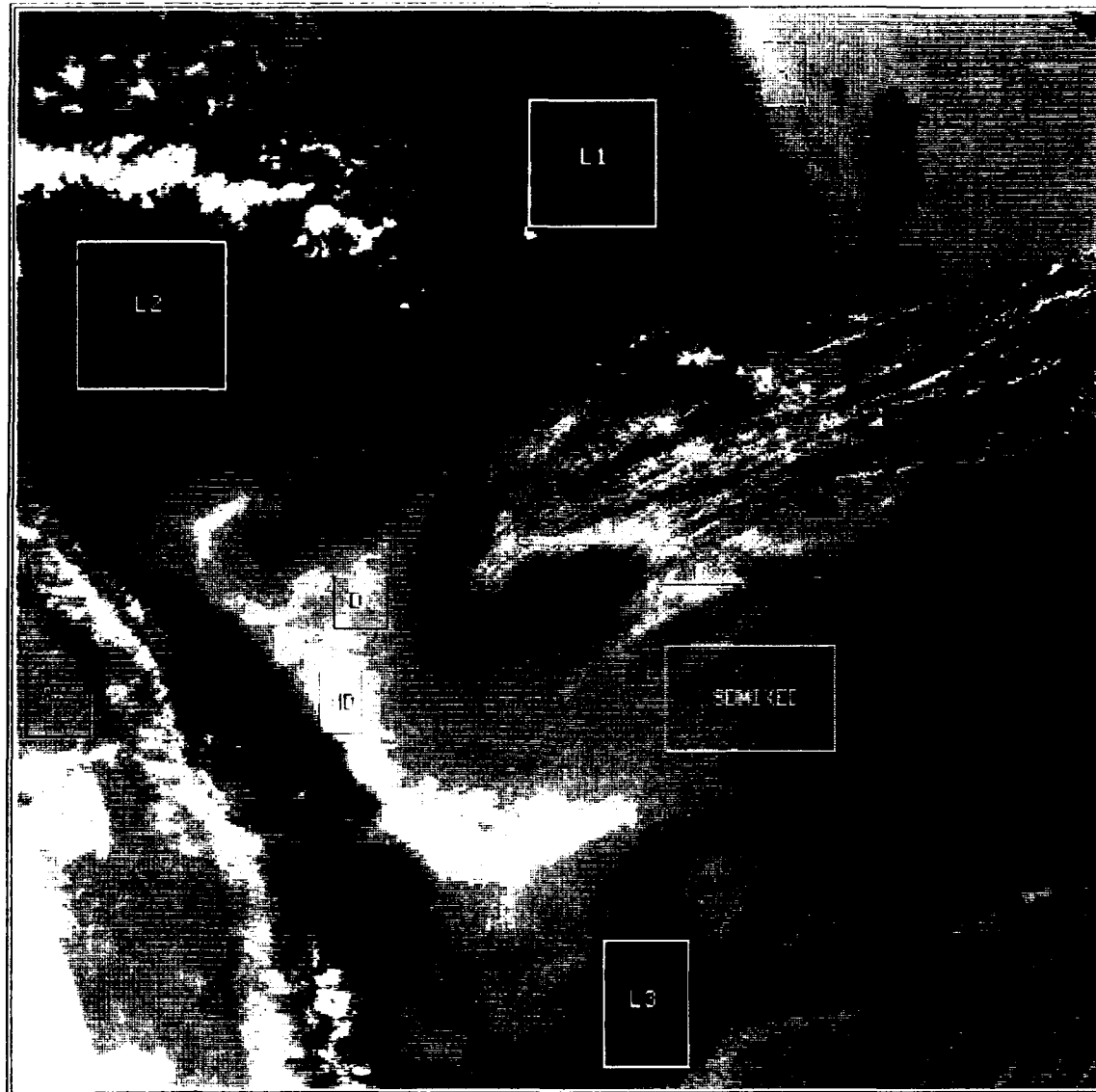


Figure 1. Aerial photograph of the study area. The image is a high-contrast, black and white aerial photograph of a coastal area, likely a bay or inlet. The image is heavily textured with dark, swirling patterns representing water and lighter, irregular shapes representing land or ice. Several rectangular boxes are overlaid on the image, each containing a label: 'L1' in the upper center, 'L2' in the upper left, 'L3' in the lower center, 'NO' in the middle left, '10' in the middle left, 'EDMIRAL' in the middle right, and 'L3' in the lower right. The overall appearance is grainy and high-contrast, typical of a photocopy of a satellite or aerial photograph.

The primary goal of this paper, as stated in the introduction, is to identify the radiative signatures of smoke and dust. Therefore, only dust, smoke, high dust and smoke/dust mixed are strictly analyzed in the following scatter plot analyses. Much of the Upper Gulf discussion concerning the land and water radiative signatures is applicable here, however.

For clarification, "dust" refers to low altitude dust and "high dust" refers to high altitude dust. Additionally, the "smoke" area analyzed on the Arabian Peninsula images is similar in location to the "thin smoke over land" area analyzed in the Upper Gulf images. A number of image combinations (cases) were generated. The following cases are the most illuminating.

**1. Case 1 Scatter Plot Analysis: Cal 2 versus Temp 3
(Figure 24)**

This image combination was selected because it highlights the significant difference in solar reflectance between smoke and dust.

a. Dust:

Dust ranges from 25.5 to 30.2 percent albedo on the Cal 2 axis and from 320.8° K to 321.8° K on the Temp 3 axis. The relatively high albedo is consistent with the general dust characteristics previously discussed in Chapter II. The temperatures in channel 3, however, are anomalously high. In

IMAGE CLASSIFICATION

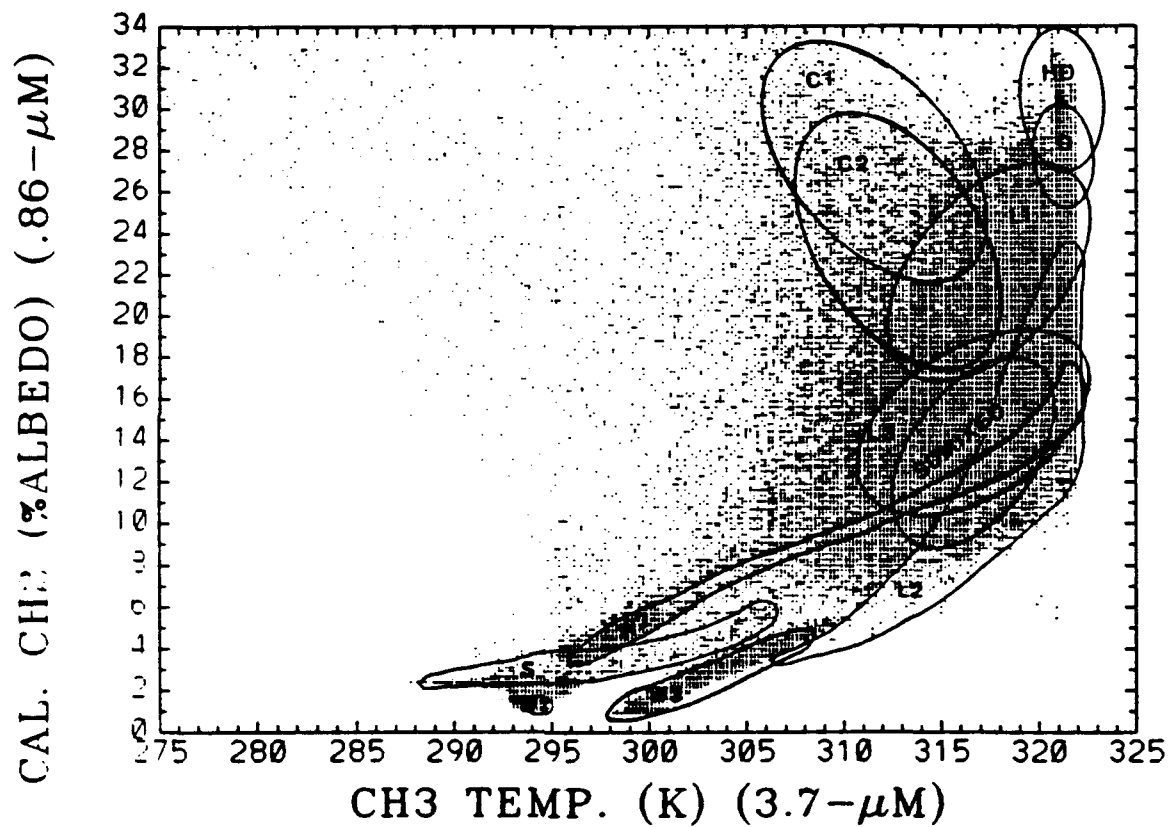


Figure 24. Case 1 Arabian Peninsula scatter plot. Feature designation corresponds with sample areas in Figure 23.

Carlson and Benjamin's (1980) idealized case for Saharan dust, it can be inferred that dust at $3.7\mu\text{m}$ has a high optical depth, small imaginary index of refraction ($\sim .01$), and high single scatter albedo. These characteristics agree with the channel 3 temperature signature in this case. The dust temperature is being driven abnormally high by the large reflective component unaccounted for in the brightness temperature. It is highly unlikely the temperature at the top of the dust plume is 39°C .

b. High Dust:

High dust ranges from approximately 26.5 to 34.0 percent albedo on the Cal 2 axis and from 320.6°K to 321.8°K on the Temp 3 axis. The slightly higher albedo, compared to that of lower altitude "dust", may be attributed to two factors. First, it is reasonable to assume the high dust consists of generally smaller particles than lower level dust. Consistent with Mie scattering theory, decreasing particle size while keeping other parameters relatively constant has the effect of increasing upwelled radiation (Kidder and Vonder Haar, 1991). Second, the area of the high dust is several hundred kilometers down wind of the plume source. Thus, it is likely there is more wind generated aerosol/dust in the air under the high dust. This implies a greater dust optical depth and therefore a greater chance for light scattered into the dust to be scattered back out toward the sensor.

Scattering of visible light by dust vice absorption is consistent with its low imaginary index of refraction at $.86\mu\text{m}$ as indicated by Figure 2. The Temp 3 brightness temperatures are anomalously high and the reasons are in line with those discussed previously for "dust".

c. Smoke:

Smoke ranges from approximately 2.3 to 6.0 percent albedo on the Cal 2 axis and from 287°K to 306.7°K on the temp 3 axis. These ranges are as expected. The reasons for this signature characteristic were discussed in the Upper Gulf analysis.

d. Smoke/Dust Mixed:

Smoke/dust mixed ranges from approximately 9.3 to 20.0 percent albedo on the Cal 2 axis and from 312.8°K to 320°K on the Temp 3 axis. This signature exhibits the characteristics of both smoke and dust. However, because of the relatively high albedos and temperatures, it appears the signature is dominated by the dust and/or the desert sand surface.

e. Summary:

This scatter plot emphasizes the significant difference in reflectance characteristics between smoke and dust. Not only does smoke have a much lower albedo but its increase in channel 3 brightness temperature is not as linearly linked to increasing channel 3 reflectance component.

Dust, on the other hand, has a relatively high albedo and its high channel 3 brightness temperature is almost strictly influenced by the large channel 3 reflective component. The relationship is at least linear if not exponential. That is difficult to discern, however, because the AVHRR channel 3 wavelength band upper limit restricts the detection of features warmer than about 322°K. That limitation accounts for the "bunching" of pixels vertically at 322°K on the scatter plot. Overall, the scatter plot distinguishes albedo signatures well but radically exaggerates "blackbody" temperatures. Additionally, even though clouds are not strictly analyzed, this image combination gives a clear separation between clouds and dust (high and low).

**2. Case 2 Scatter Plot Analysis: Cal 2 versus Temp 4
Figure 25)**

There are various features in the Arabian Peninsula area (ie., dust, desert sand, clouds, etc.) that have similar solar reflectance characteristics. This image combination is used to discriminate between those features by its blackbody temperature.

a. Dust:

Dust ranges from 25.5 to 30.2 percent albedo on the Cal 2 axis and from 283°K to 288.8°K on the Temp 4 axis. The Cal 2 range is in agreement with case 1. The Temp 4 range is significantly different from the Temp 3 range for dust (33°K

IMAGE CLASSIFICATION

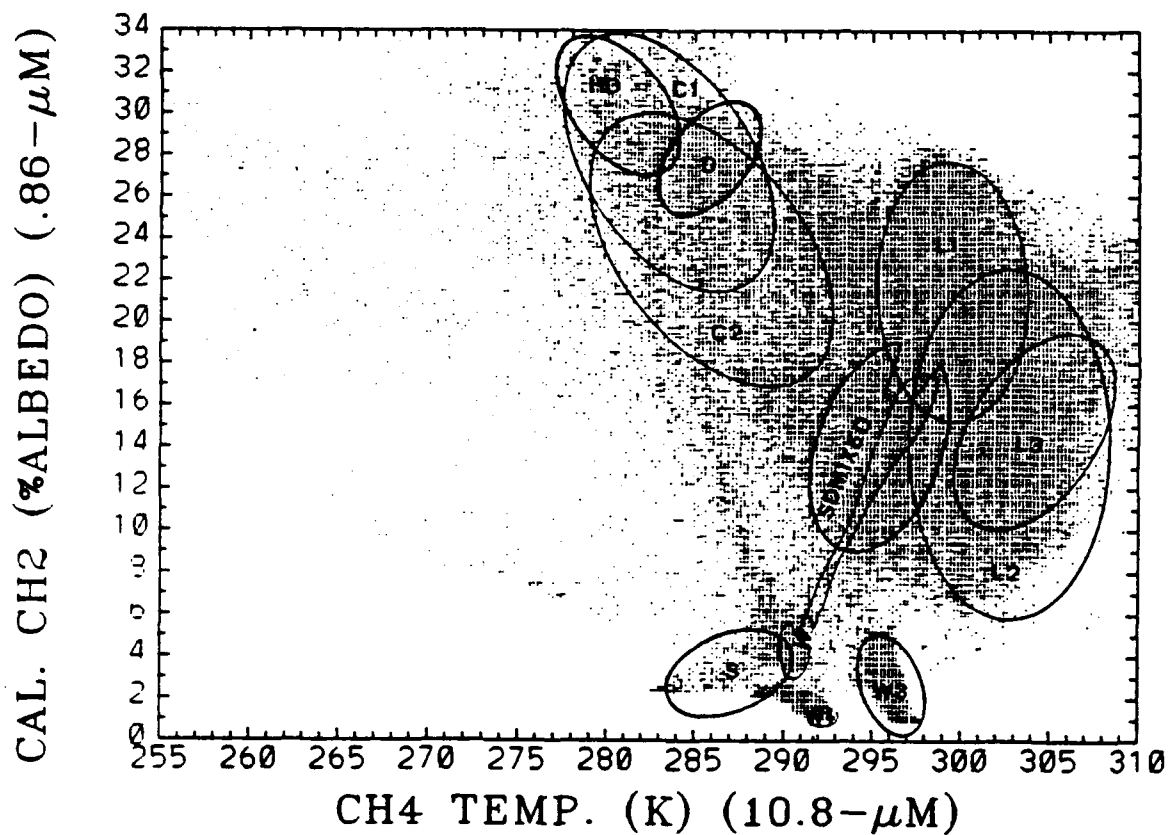


Figure 25. Case 2 Arabian Peninsula scatter plot. Feature designation corresponds with sample areas in Figure 23.

to 39°K difference). As indicated in Figure 2, dust has an order of magnitude higher imaginary index of refraction at 10.8 μ m than at 3.7 μ m. That essentially makes it more of a "blackbody" in channel 4 than in channel 3. For this reason the Temp 4 range is more representative of the temperature at the top of the lower dust plume.

b. High dust:

High dust ranges from approximately 26.5 to 34.0 percent albedo on the Cal 2 axis and from 277.7°K to 283.5°K on the Temp 4 axis. The Cal 2 range is consistent with case 1. Once again, the Temp 4 range is indicative of the true temperature of the high dust plume as compared to the Temp 3 range. The cooler temperatures compared to the lower dust are primarily altitude related. As previously stated, dust absorbs 10.8 μ m wavelength energy very well. Referring to Figure 26, it indicates the sun radiates little to no radiation at the 10.8 μ m wavelength. Therefore, the plume top dust is getting most of its 10.8 μ m energy from the atmosphere and so its temperature is representative of the atmospheric temperature at its particular altitude. Note that even though 10.8 μ m is in a water vapor window, the sounding from Riyadh, Figure 6 shows a very dry atmosphere. This translates to little contribution by water vapor thermal emission to

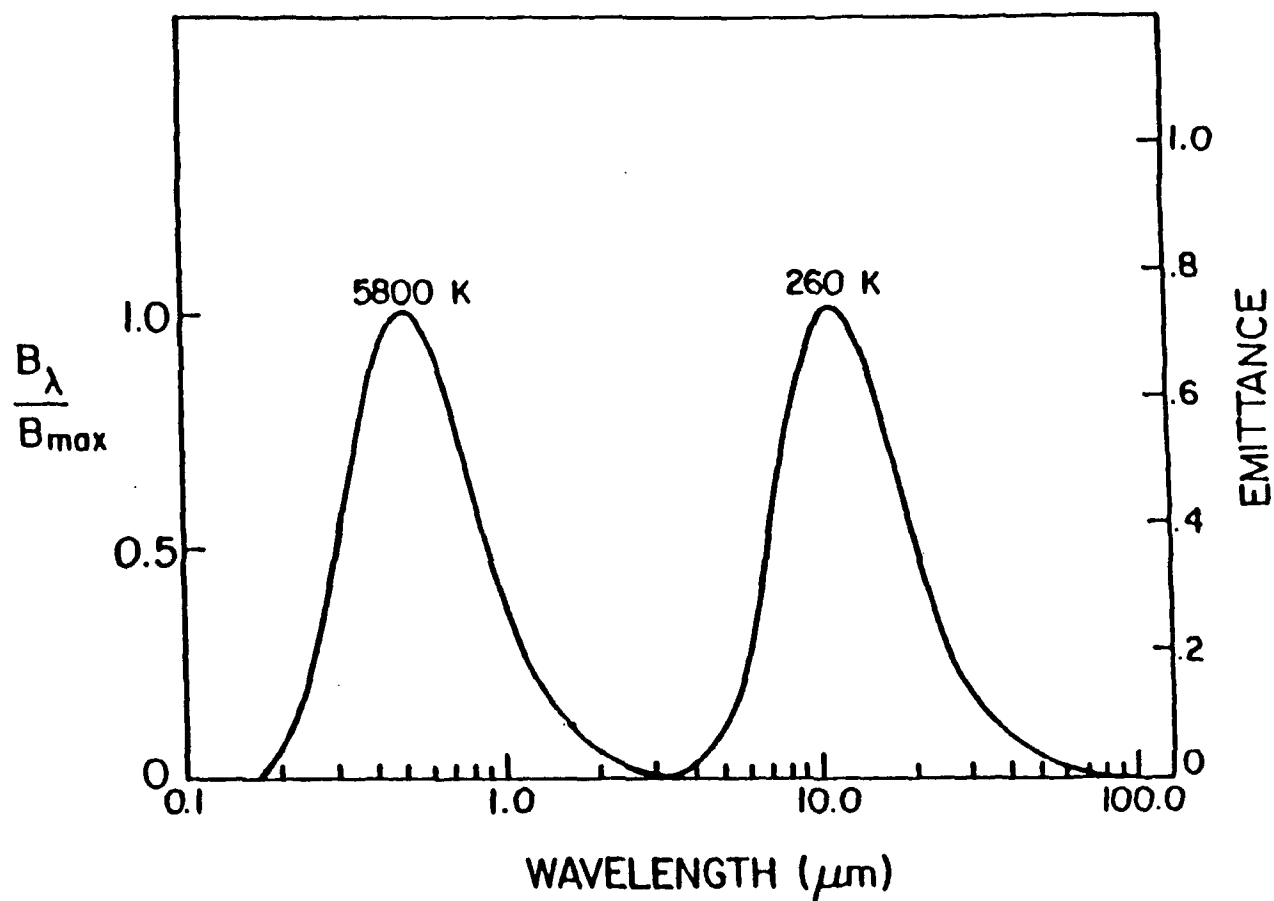


Figure 26. Normalized Planck curves representing solar radiation (5800K) and terrestrial radiation (260K) by wavelength (μm). adapted from Kidder and Vonder Haar, 1992)

atmospheric temperature, further justifying Temp 4 plume top temperatures as indicative of atmospheric temperature.

c. Smoke:

Smoke ranges from approximately 2.3 to 6.0 percent albedo on the Cal 2 axis and from 283.5°K to 290.8°K on the Temp 4 axis. The Cal 2 range is consistent with case 1 and the Upper Gulf smoke albedo discussion applies. The Temp 4 range is representative of thin smoke over land/water as indicated in the Upper Gulf cases. The highest temperatures represent thin smoke over water and the lower and temperatures represent thin smoke over land. The reasoning is also the same as in the Upper Gulf analyses.

d. Smoke/Dust Mixed:

Smoke/dust mixed ranges from 9.3 to 20.0 percent albedo on the Cal 2 axis and from 291.5°K to 299°K on the Temp 4 axis. The Cal 2 range is consistent with case 1. The Temp 4 range is most representative of actual temperatures as compared to Temp 3. The signature discussion for albedo and temperature from case 1 is applicable here.

e. Summary:

Overall, this scatter plot depicts excellent signature separation between the four analyzed features. A final footnote, because Temp 4 has little reflective component in its brightness temperatures, the dust signature is almost all due to thermal emission and therefore most indicative of

its actual blackbody temperature and for reasons discussed previously, that of the atmosphere. There is, however, some ambiguity between the dust and cloud signatures as can be seen by the overlapping ovals on the scatter plot (Figure 25). This indicates an unambiguous representation of the dust distribution cannot be achieved when clouds are present using this image combination.

3. Case 3 Scatter Plot Analysis: Cal 2 Versus Temp 5 (Figure 27)

This parameter combination was selected, primarily to investigate the difference in feature thermal emission between channels 4 and 5. All Cal 2 ranges are the same as previous cases. Therefore, only the Temp 5 signature ranges will be identified/ discussed.

a. Dust:

Dust ranges from approximately 283.8°K to 289.8°K on the Temp 5 axis. These temperatures are slightly higher (~1°K) than in Temp 4 which alludes to an important dust characteristic. It implies dust is a better absorber/emitter of channel 4 IR wavelengths (10.8μm). This is substantiated by Figure 3 from which a higher imaginary index of refraction can be inferred for channel 4 compared to channel 5. Because of this difference in absorption, the dust is not as optically thick in channel 5 compared to channel 4 and thus channel 5 detects more thermal emission from the warmer surface. This

accounts for the slightly higher channel 5 brightness temperatures. Additionally, note in Figure 28 that channel 4 lies more in a water vapor window than channel 5. Therefore, channel 5 brightness temperatures are more sensitive to water vapor thermal emissions. Sounding data previously referenced, however, indicates a relatively dry atmosphere over the region; so the water vapor influence is most likely small. That is primarily speculation, however, because it is based on such sparse sounding data.

b. High Dust:

High dust ranges from 278.2°K to 285°K on the Temp 5 axis. Once again the temperatures are slightly higher (.5°K to 1.5°K) than in Temp 4. The previous "dust" discussion as well as the discussion in case 2 for high dust apply here.

c. Smoke:

Smoke ranges from approximately 283.5°K to 290.8°K on the Temp 5 axis. This is consistent with the range analyzed in Temp 4, thus indicating no significant difference in smoke signature between the two channels. Therefore, the discussion in case 2 is applicable here.

IMAGE CLASSIFICATION

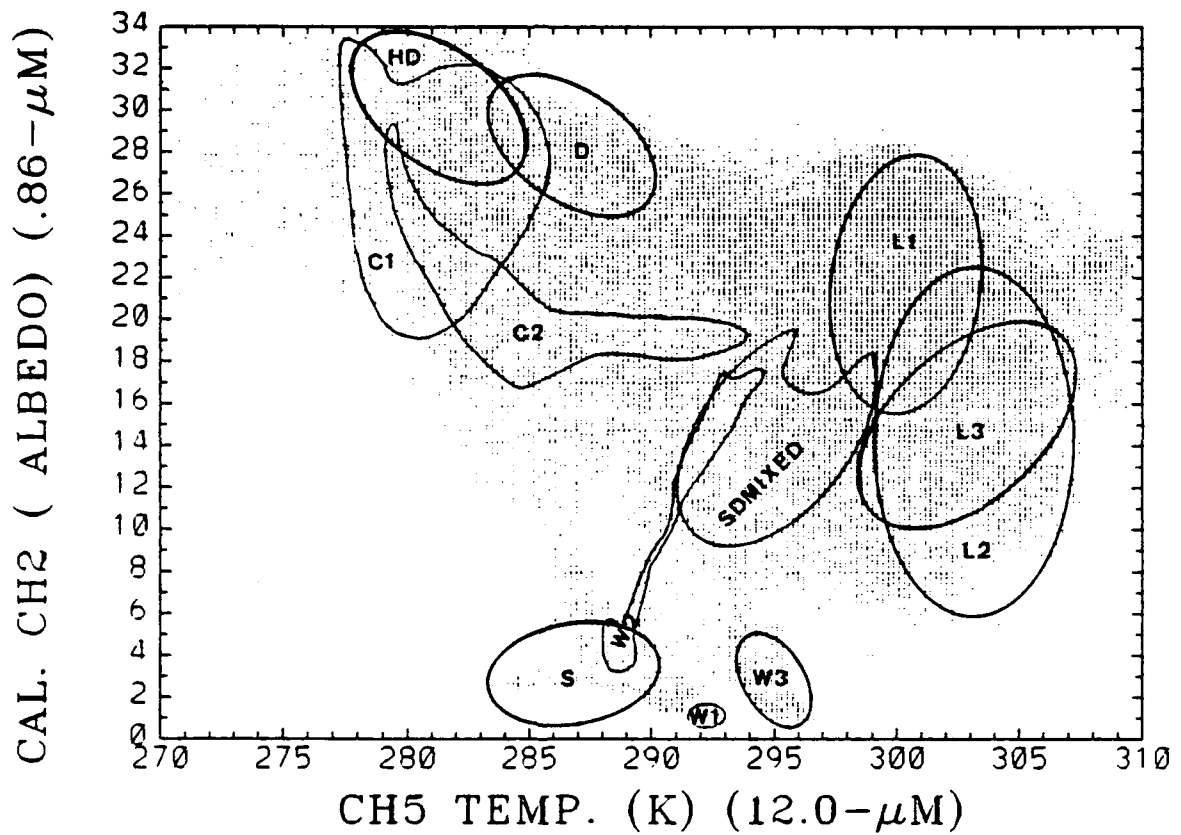


Figure 27. Case 3 Arabian Peninsula scatter plot. Feature designation corresponds with sample areas in Figure 23.

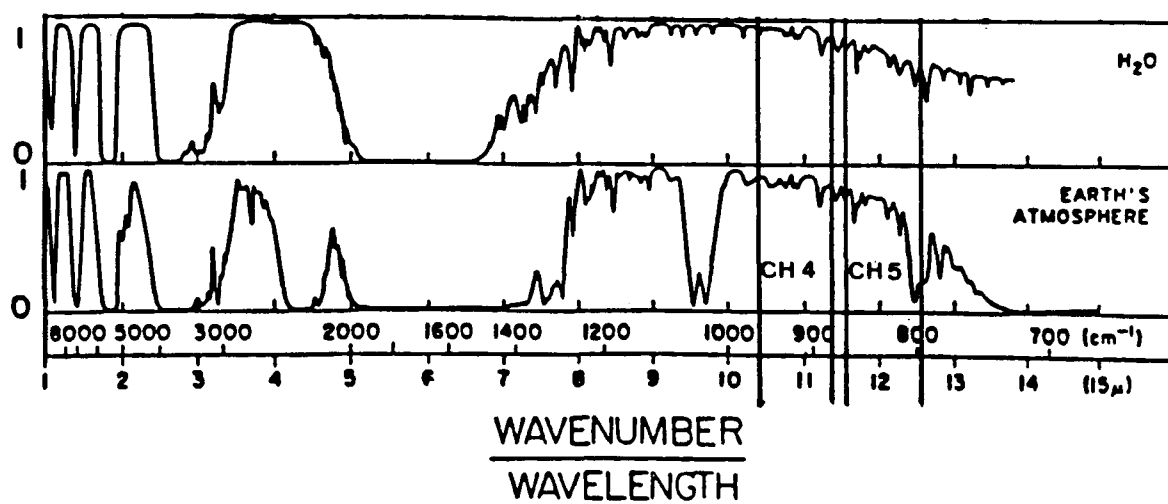


Figure 28. Infrared water vapor (H₂O) transmittance. Water vapor "window" is between 8-12 μ m. (Adapted from Kidder and Vonder Haar, 1992.) The AVHRR/1 channel 4 and channel 5 wavelength bands are delineated.

d. Smoke/Dust Mixed:

Smoke/dust mixed ranges from 291.5°K to 299°K on the Temp 5 axis. This is the same range as in Temp 4 and that discussion from case 2 applies here.

e. Summary:

Overall, this scatter plot depicts the same information as in case 2. Of particular note again, is the ambiguity in signature between the dust and clouds. However, the one key difference is the higher temperature of the dust compared to Temp 4. This indicates dust is a slightly better "blackbody" in channel 4 than in channel 5. Therefore, channel 4 temperatures are probably more representative of the dust plume temperatures.

**4. Case 4 Scatter Plot Analysis: Cal 2 versus T4-T5
(Figure 29)**

This parameter combination was selected to investigate the different dust absorption characteristic between channels 4 and 5. All Cal 2 ranges are the same as previous cases. Therefore, only the T4-T5 signature ranges will be identified/discussed.

IMAGE CLASSIFICATION

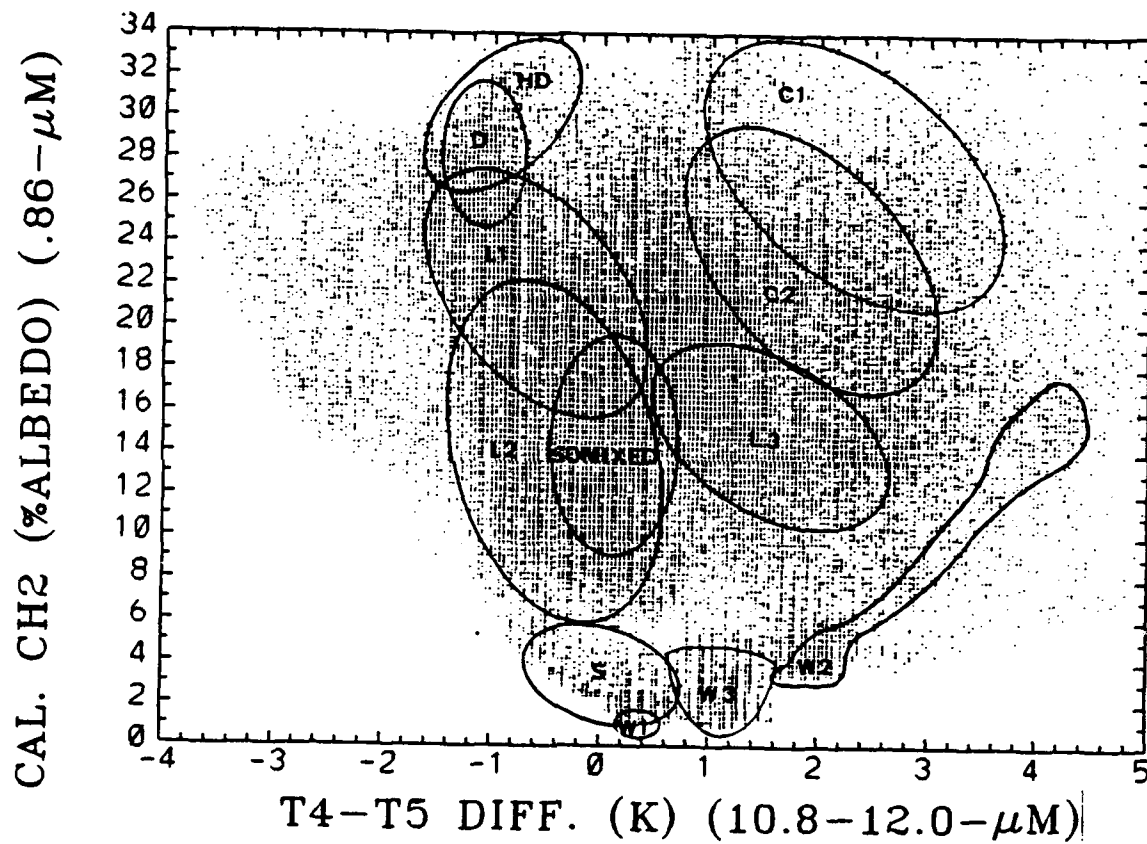


Figure 29. Case 4 Arabian Peninsula scatter plot. Feature designation corresponds to sample areas in Figure 23.

a. Dust:

Dust ranges from approximately -0.8°K to -1.47°K temperature difference on the T4-T5 axis. The negative difference for the dust signature is expected. The reasons for the difference were discussed in case 3.

b. High Dust:

High dust ranges from approximately $-.35^{\circ}\text{K}$ to -2.1°K temperature difference on the T4-T5 axis. The reasons for the negative differences were discussed in case 3.

c. Smoke:

Smoke ranges from approximately -3.2°K to $+3.2^{\circ}\text{K}$ temperature difference on the T4-T5 axis. The smoke is centered about zero which emphasizes its neutrality between channels 4 and 5. The positive difference is influenced by gulf water thermal emission and indicates channel 4's higher sensitivity to those emissions. The negative difference is influenced by the land thermal emissions and alludes to channel 5 being more sensitive to those emissions.

d. Smoke/Dust Mixed:

Smoke/dust ranges from approximately -1.8°K to $+2.1^{\circ}\text{K}$ temperature difference on the T4-T5 axis. This signature appeals to the neutrality of smoke and the albedo of a sand surface and/or dust. It is a complex signature and the location of the sample are on the scatter plot supports the

hypothesis of a smoke/dust and sand surface signature combination.

e. Summary:

The primary significance of this scatter plot is that it emphasizes and quantifies the difference in dust signature between Temp 4 and Temp 5. The quantification allows for exploitation of the signature difference to locate dust outbreaks. Note on the scatter plot (Figure 29), however, there is a slight overlap between the dust and land areas 1 (L1). This may pose some ambiguity in determining the dust distribution.

**5. Case 5 Scatter Plot Analysis: T3-T4 versus Cal 2
(Figure 30)**

This image combination was selected to investigate the effect of the solar reflectance component in channel 3 on feature brightness temperature. The Cal 2 ranges are as analyzed in case 1.

a. Dust:

Dust ranges from approximately 32.5°K to 38.0°K temperature difference on the T3-T4 axis. The large positive difference values are indicative of the huge influence of the channel 3 reflective component on the brightness temperature of the dust. This large influence proves effective, however, in distinguishing the dust signature from the other features

IMAGE CLASSIFICATION

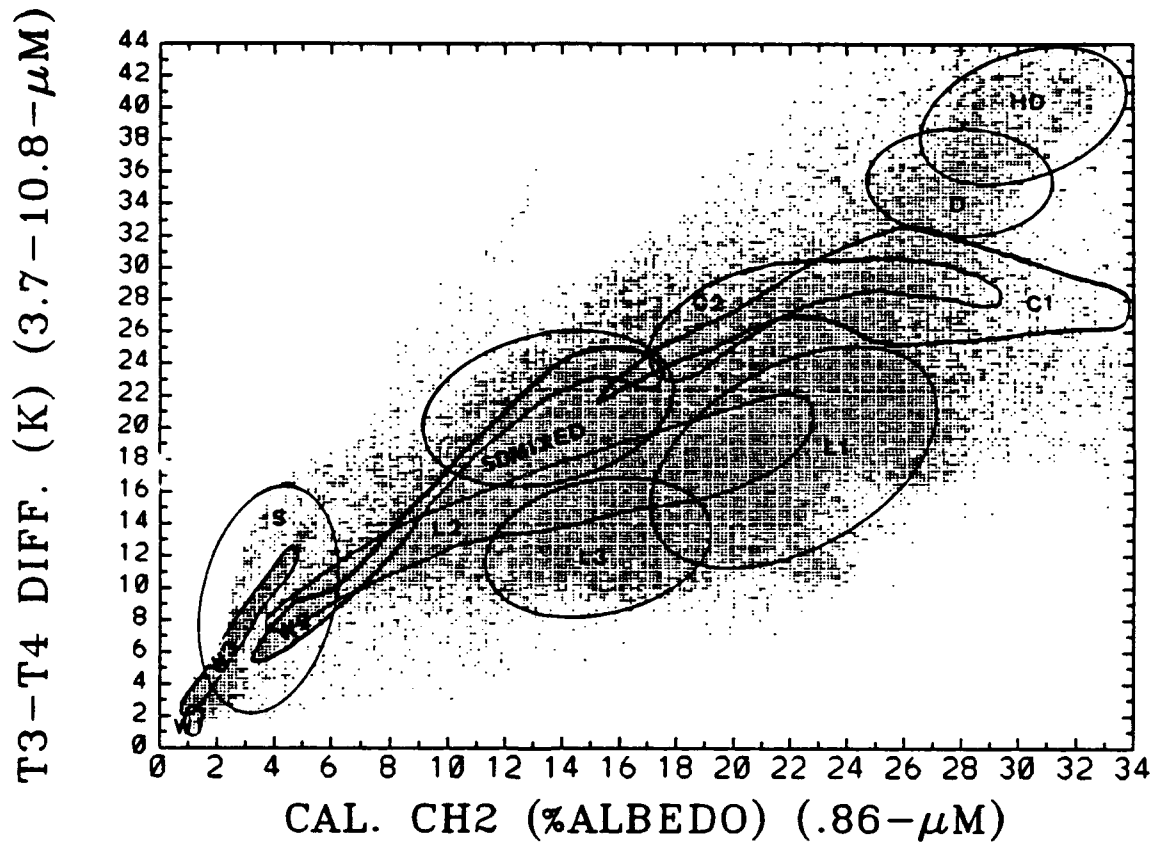


Figure 30. Case 5 Arabian Peninsula scatter plot. Feature designation corresponds to sample areas in Figure 23.

when plotting it against its high albedo in channel 2. And unlike case 1, the upper channel 3 brightness temperature limit does not hinder the scatter plot from representing the true relationship between the reflective component of the channel 3 brightness temperatures and the Cal 2 albedos.

b. High Dust:

The high dust ranges from approximately 38.0°K to 43.0°K temperature difference on the T3-T4 axis. As with the lower "dust", the large temperature difference influenced by the reflective component in the channel 3 brightness temperatures enhances the signature and creates excellent separation from the other features.

c. Smoke:

Smoke ranges from approximately 2.5°K to 16.0°K temperature difference on the T3-T4 axis. This is consistent with the ranges and discussion for thin smoke over land/water in the Upper Gulf analyses.

d. Smoke/Dust Mixed:

Smoke/dust mixed ranges from approximately 18.0°K to 25.0°K temperature difference on the T3-T4 axis. This once again is consistent with a signature representative of a combination of smoke and dust and/or sand surface.

e. Summary:

This scatter plot successfully separates the high dust and dust signatures from each other and the other

features. It is much more effective at showing the relationship between the channel 3 reflectance and channel 2 albedo.

**6. Case 6 Scatter Plot Analysis: T4-T5 versus Temp 4
(Figure 31)**

This image combination was selected because it gives excellent separation of the dust signature (both dust and high dust) from the other features on the scatter plot; the different absorption characteristic of dust between channels 4 and 5 (as previously discussed) accounts for the negative dust values on the T4-T5 axis. There are some areas of land that have negative values but because those areas are warmer than the dust, they can be separated by plotting T4-T5 versus their temperatures (ie. Temp 4), as in this case. There are also some clouds that have negative to small positive T4-T5 differences. Again, however, there is separation from dust based on temperature differences. Notice on the scatter plot, Figure 31, there is a low pixel density area (a line) running diagonally from left to right approximately from the point (275°K, +.4°K T4-T5 difference) to (303°K, -2.0°K T4-T5 difference). All pixels below that area are dust and all other features are above the area. Thus, the conclusion is this scatter plot/image combination provides the most unambiguous representation of the dust signature.

C. VERIFICATION OF SCATTER PLOT ANALYSES

As previously described in Chapter III, a two dimensional mask routine is utilized to verify the analyzed signature limits from the scatter plots. The mask was run on all cases but only the most significant cases from each area will be discussed.

1. Upper Gulf Scatter Plots

Two cases, S12L versus Temp 4 and T34 versus Temp 4, are presented for the Upper Gulf area. In both cases, only the smoke and water limits are masked. The thick smoke is in red, thin smoke over land in green, thin smoke over water in magenta and water in blue.

a. S12L versus Temp 4

Figure 32 is the scatter plot showing the boxed limits for the masked features. The limits correspond with those analyzed using the scatter plot technique. The limit selection is somewhat subjective, but notice that in this case there is relatively clear separation between features. S12L contrasts the smoke from the water and Temp 4 separates the smoke plume temperature from surface features and emphasizes the influence of surface emittance on the thin smoke radiative signatures (ie., as the smoke thins it begins to take on the signature of the surface over which it lies). Figure 33 is the mask of the limits for this scatter plot overlaid on the

IMAGE CLASSIFICATION

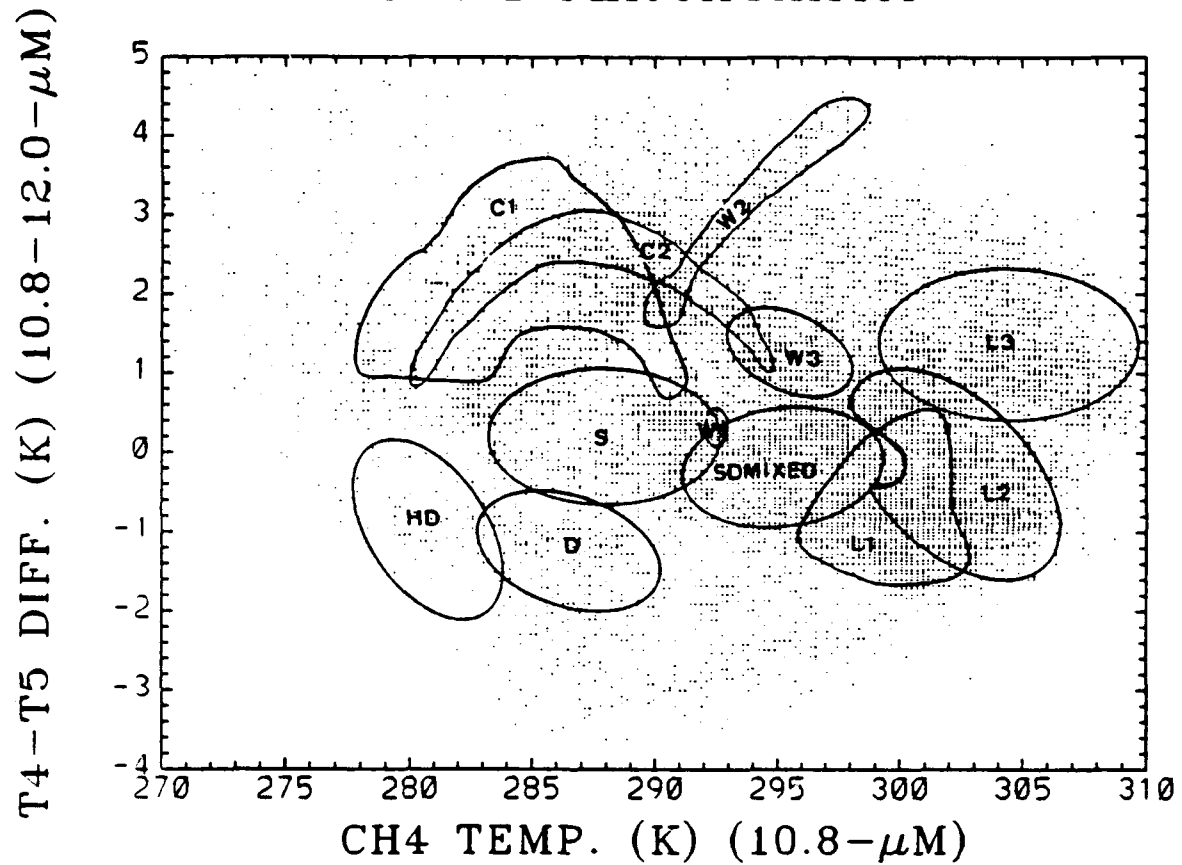


Figure 31. Case 6 Arabian Peninsula scatter plot. Feature designation corresponds to sample areas in Figure 23.

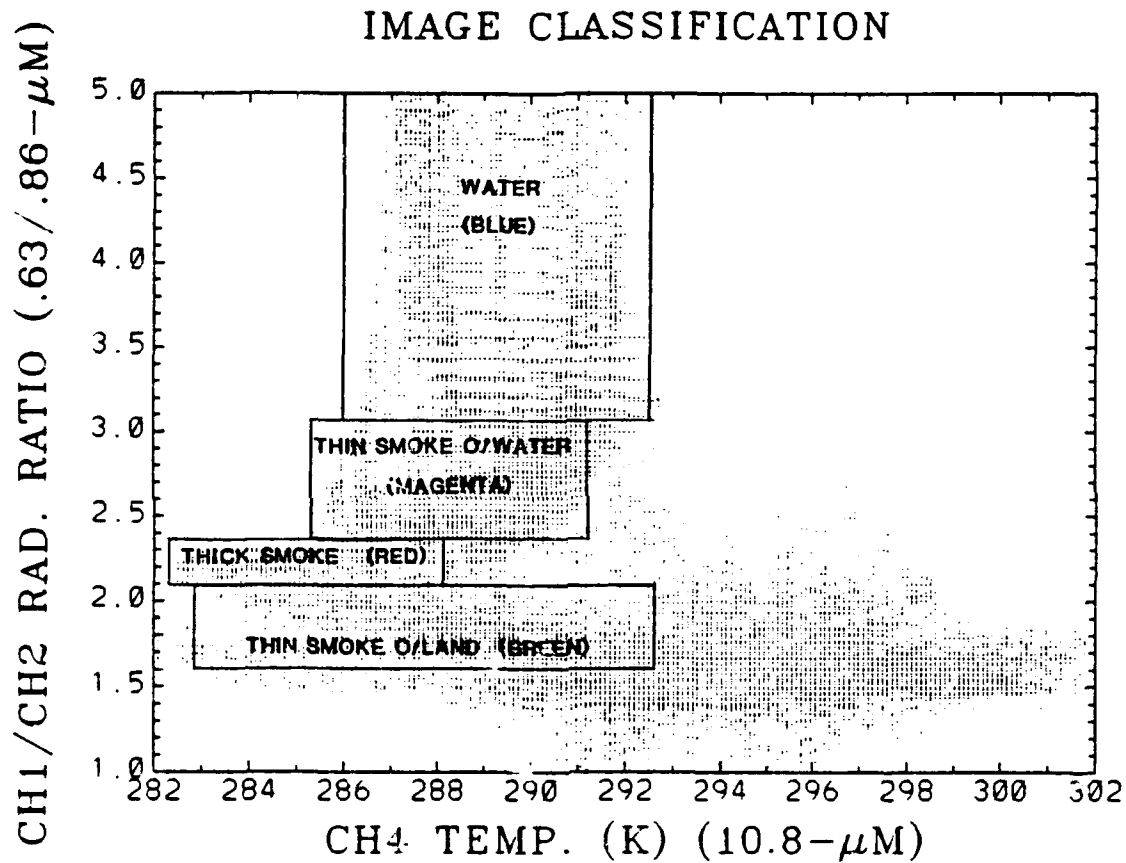


Figure 32. Analyzed 2D feature radiative signature limits for case 1 Upper Gulf scatter plot. Colors correspond to those in mask, Figure 33.

S12L satellite image. Notice the thick smoke is primarily in the center of the plume and the thin smoke is on the periphery and downwind. The mask does a good job of representing the smoke distributions over both land and most importantly, water.

b. T3-T4 versus Temp 4

Figure 34 on the T3-T4 versus Temp 4 scatter plot shows the boxed limits for the masked features. (Note: thin smoke over land is described by two limit boxes.) The second limit was added to further delineate the feature. It is represented in range on the masked image. This image combination gives good separation of the main features - water and land from the smoke. On the other hand, it also emphasizes the complexity/ambiguity of the smoke signature due to the surface type influence. This is indicated by the overlap of the smoke limits. Figure 35 is the mask of the limits overlaid on the S12L satellite image. Comparison with the previous mask, Figure 33, shows the overall smoke distribution to be approximately the same. The significant difference is between the thick smoke versus thin smoke distributions. Those limits are more ambiguous on the T3-T4 versus Temp 4 scatter plot and therefore are not as clearly masked as in the S12L versus Temp 4 case. Overall, however, it is a good representation of the smoke distribution.

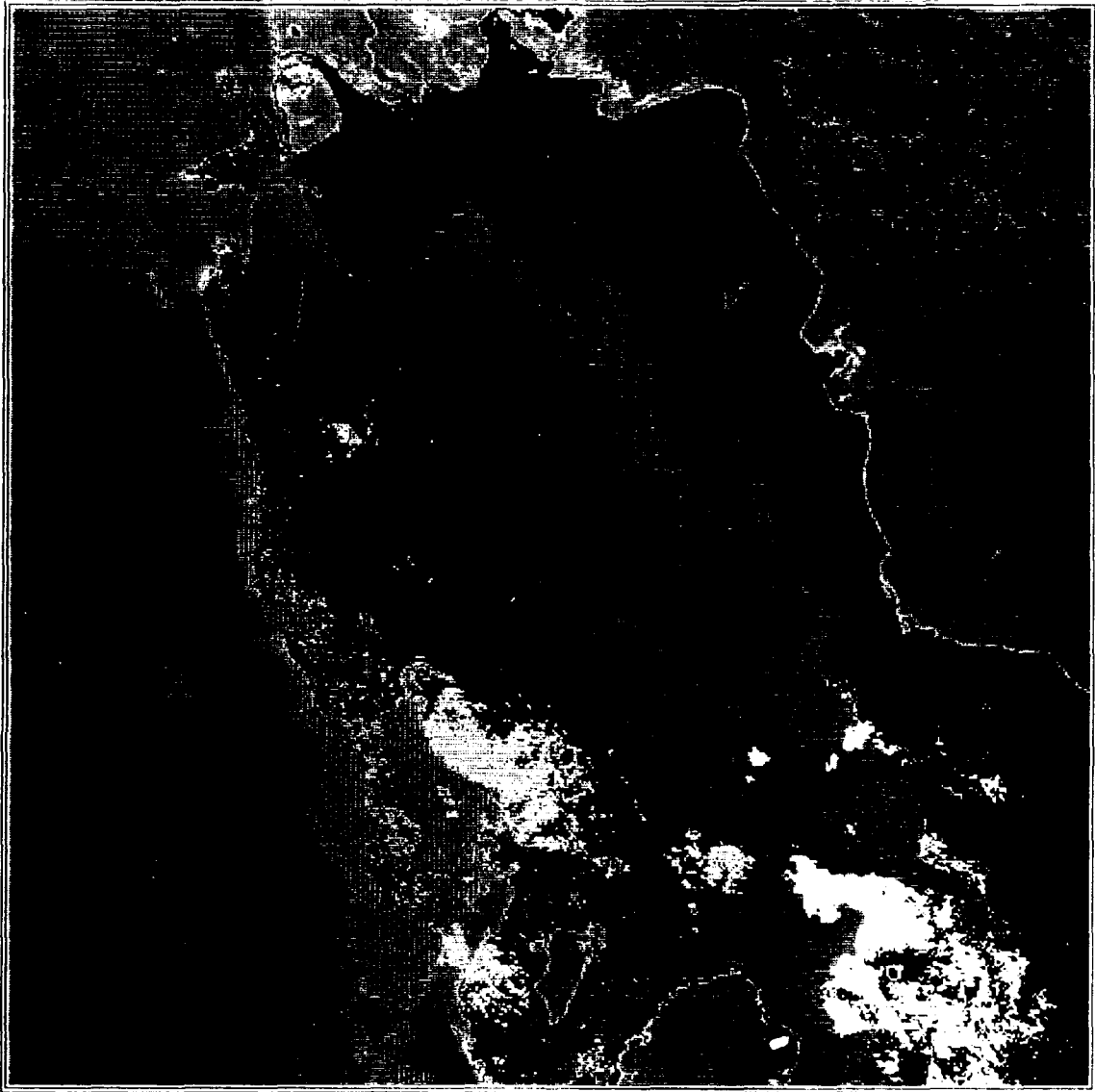


Figure 33. A dark, irregularly shaped object, possibly a rock or a piece of debris, set against a lighter, textured background. The object has a rough, jagged edge and a dark, possibly metallic or carbonaceous surface. The background is a light, grainy texture, possibly a rock face or a piece of paper. The overall image is very dark and has a high level of contrast.

IMAGE CLASSIFICATION

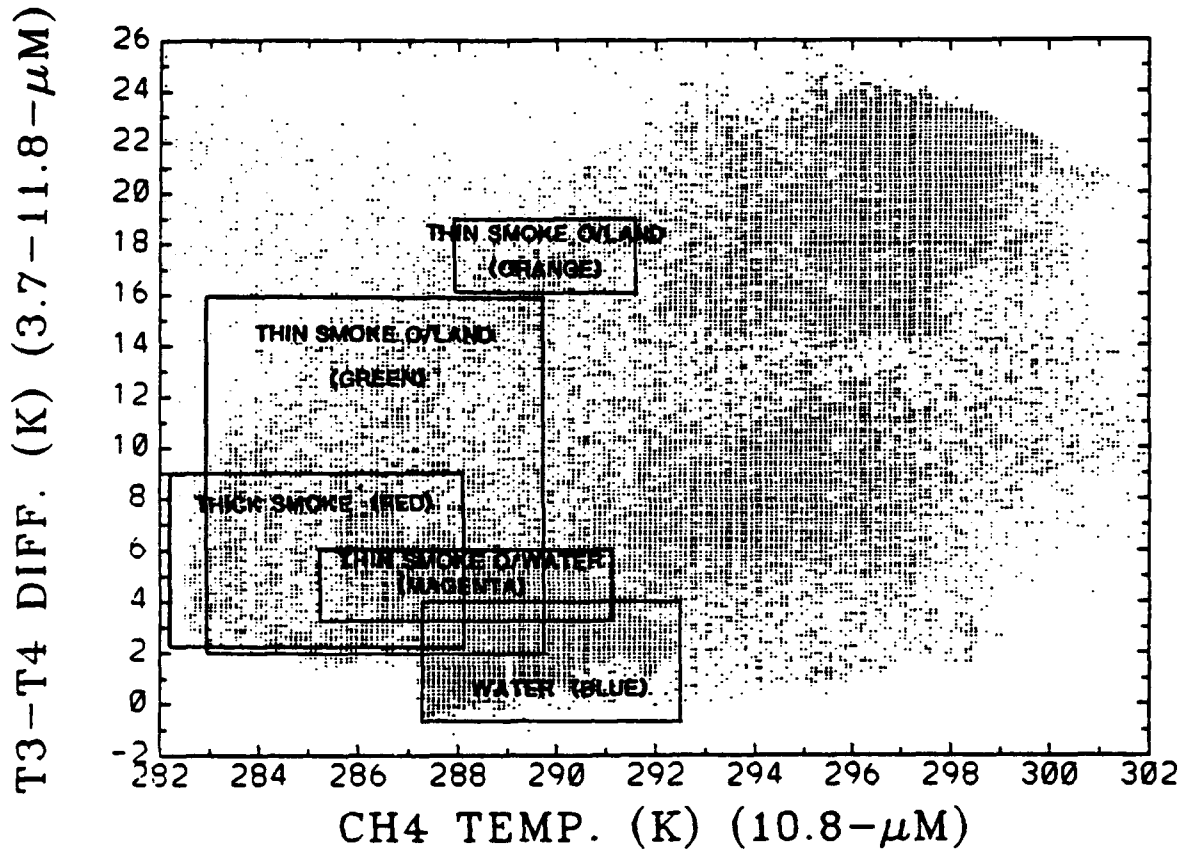


Figure 34. Analyzed 2D feature radiative signatures for Case 3 Upper Gulf scatter plot. Color corresponds to those in mask, Figure 35.



Figure 35. T1/T4 sensor Temp 4 mask utilizing limitation in Figure 34. Mask overlaid on Temp 4 image shows smoke distribution on 1 March 1991 at 1026 UTC. Red is thick smoke, green and orange are thin smoke over land, magenta is thin smoke over water and blue is water.

2. Arabian Peninsula Scatter Plots

Three cases are discussed for this area - Cal 2 versus Temp 5, Cal 2 versus T4-T5 and T4-T5 versus Temp 4. Only the dust limits are masked for each case.

a. Cal 2 versus Temp 5

Figure 36 is the scatter plot depicting the limit boxes for low dust and high dust. The difference between low dust and high dust is based on temperature with low dust being warmer. The mask of these limits, Figure 37, represents low dust in red and high dust in yellow with the Temp 5 satellite image underlaid. The mask, however, is somewhat ambiguous in representing the dust areas. Referring to the Cal 2 (Figure 38) and Temp 5 (Figure 39) satellite images, some of the clouds, as well as some of the coastal land areas along the Red Sea and Arabian Sea, have the same signature as the dust in both images; they are masked along with the dust. Therefore, even though the dust plume is represented, it is not done so unambiguously.

b. Cal 2 versus T4-T5

Figure 40 is the scatter plot depicting the limit boxes. In this case, the dust limits were subdivided into four regions. This gives better resolution and depiction of the dust distributions. Referring to the Cal 2 (Figure 41) and T4-T5 (Figure 42) satellite images, it can be seen parts

IMAGE CLASSIFICATION

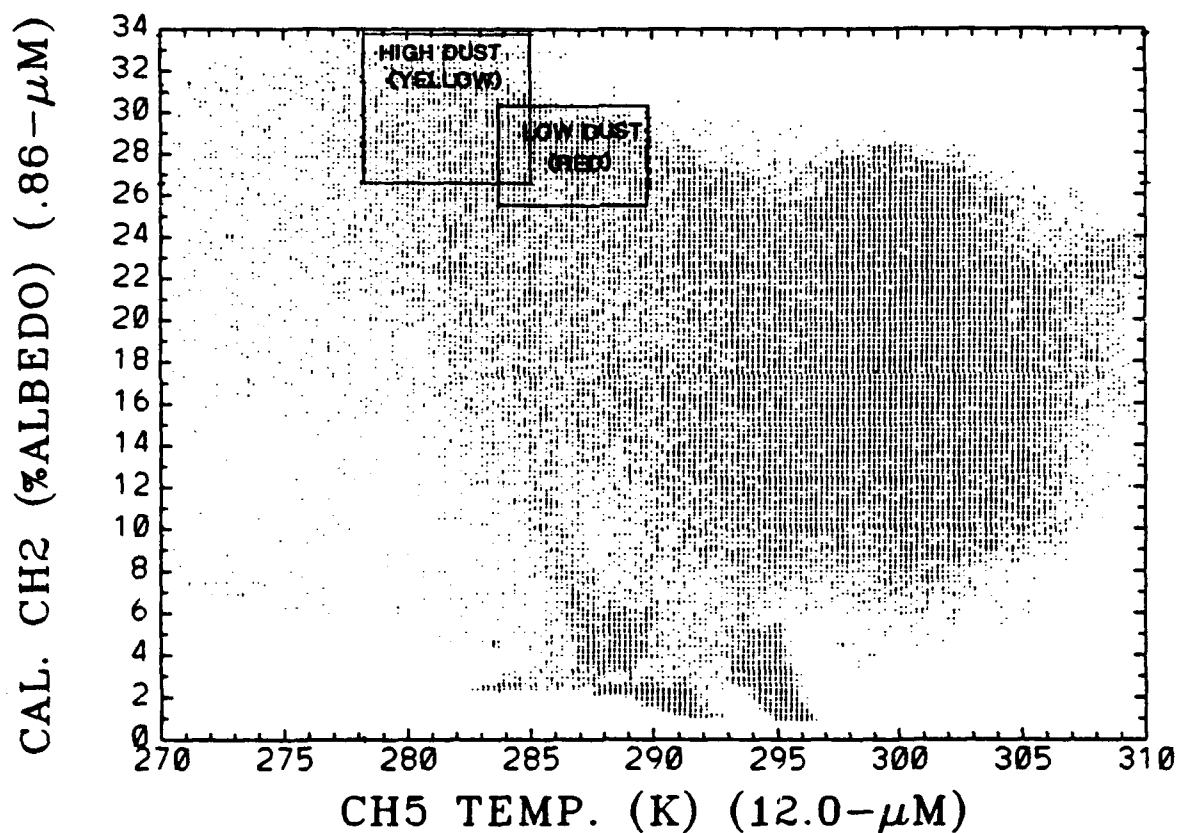


Figure 36. Analyzed 2D "dust" radiative signature for Case 3 Arabian Peninsula scatter plot. Colors correspond to those in mask, Figure 37.

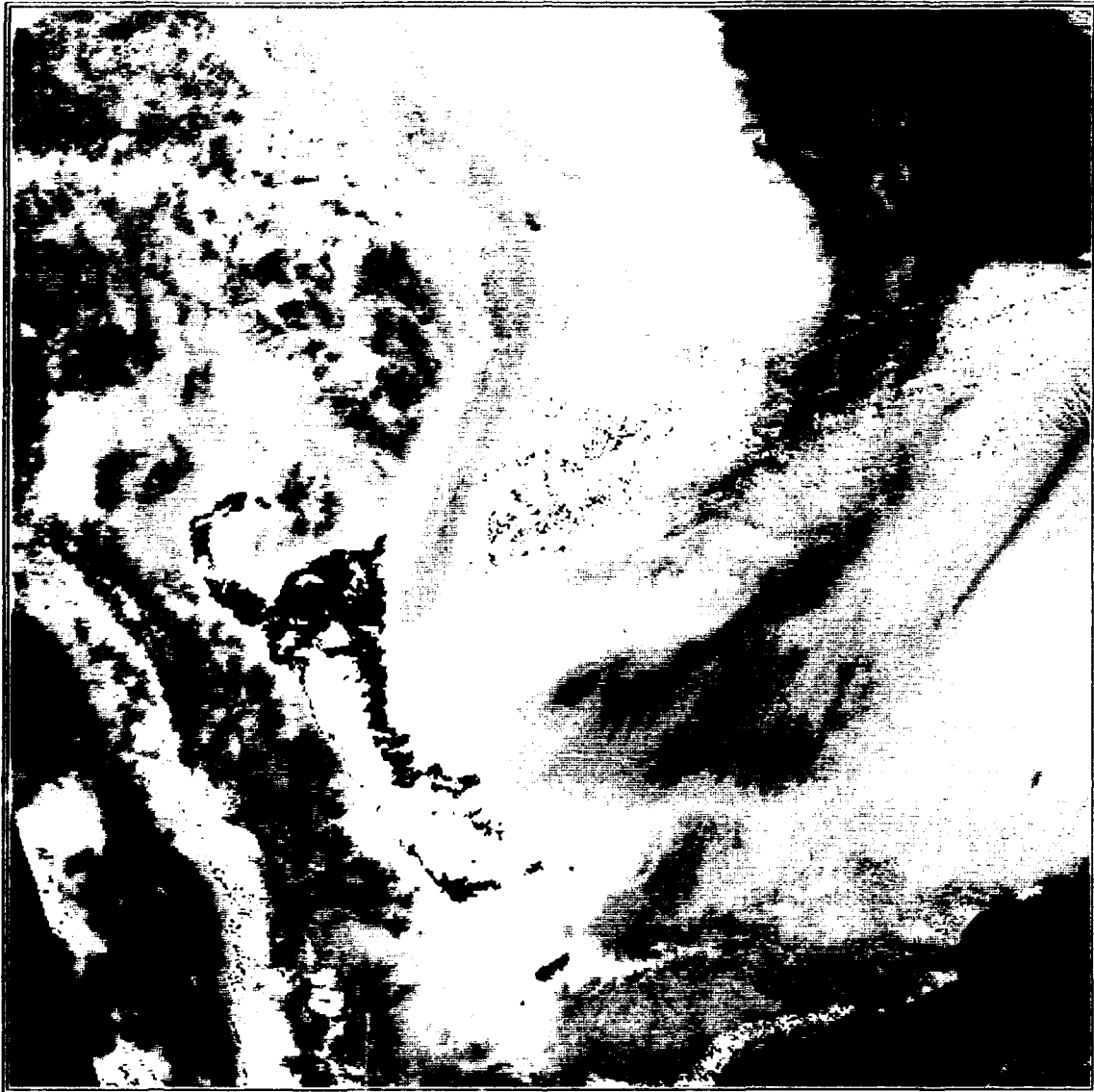


Figure 37. Cal 2 versus Temp 5 mask utilizing limits in Figure 36. Mask overlaid on Cal 2 image shows approximate dust plume distribution. There is some ambiguity between dust plume, clouds and coast.

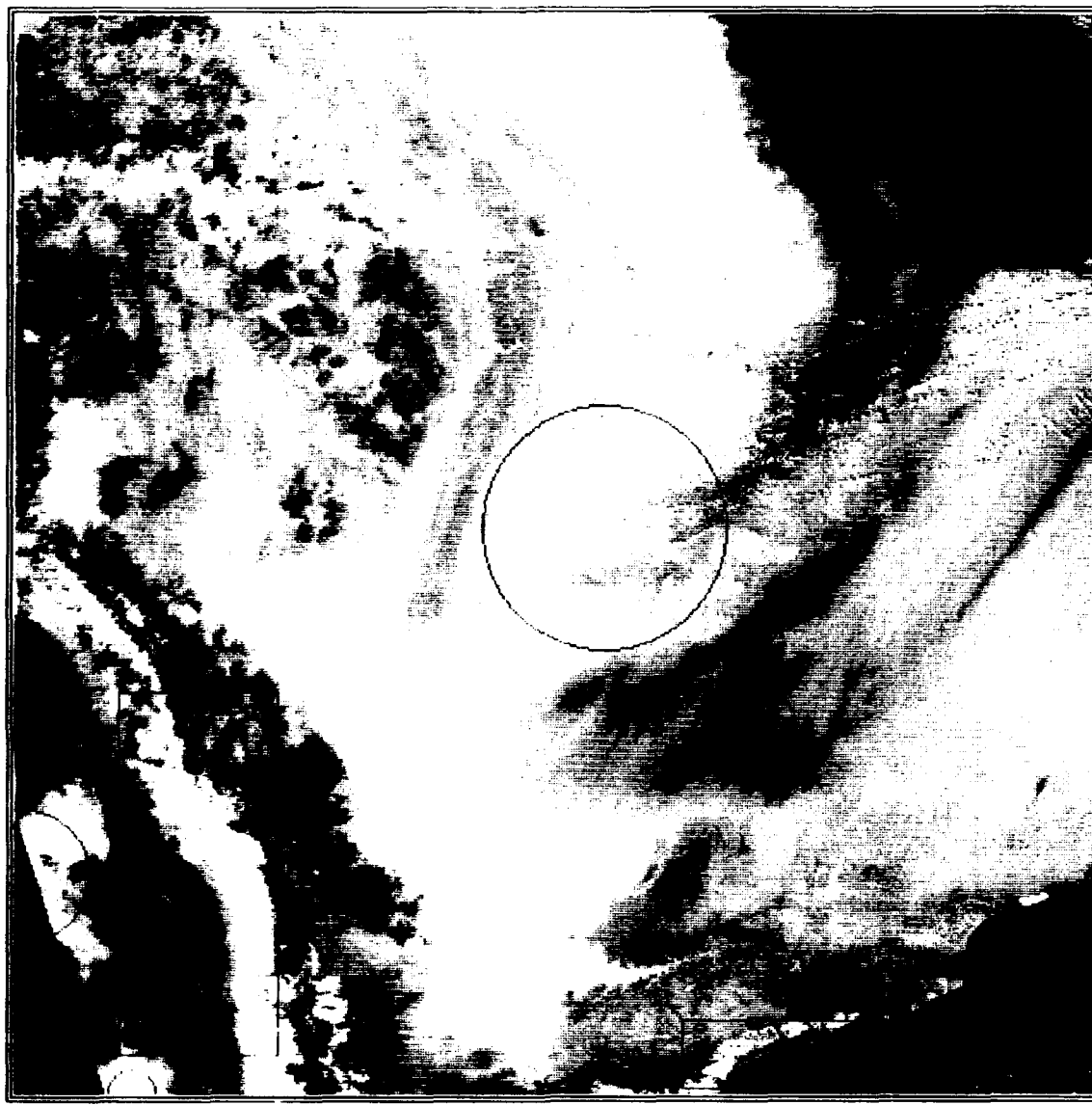


Figure 38. Cal 2 1 March 1991 1026 UTC Arabian Peninsula image. Some clouds (circles) and coastal land (rectangles) have similar brightness as dust plume.

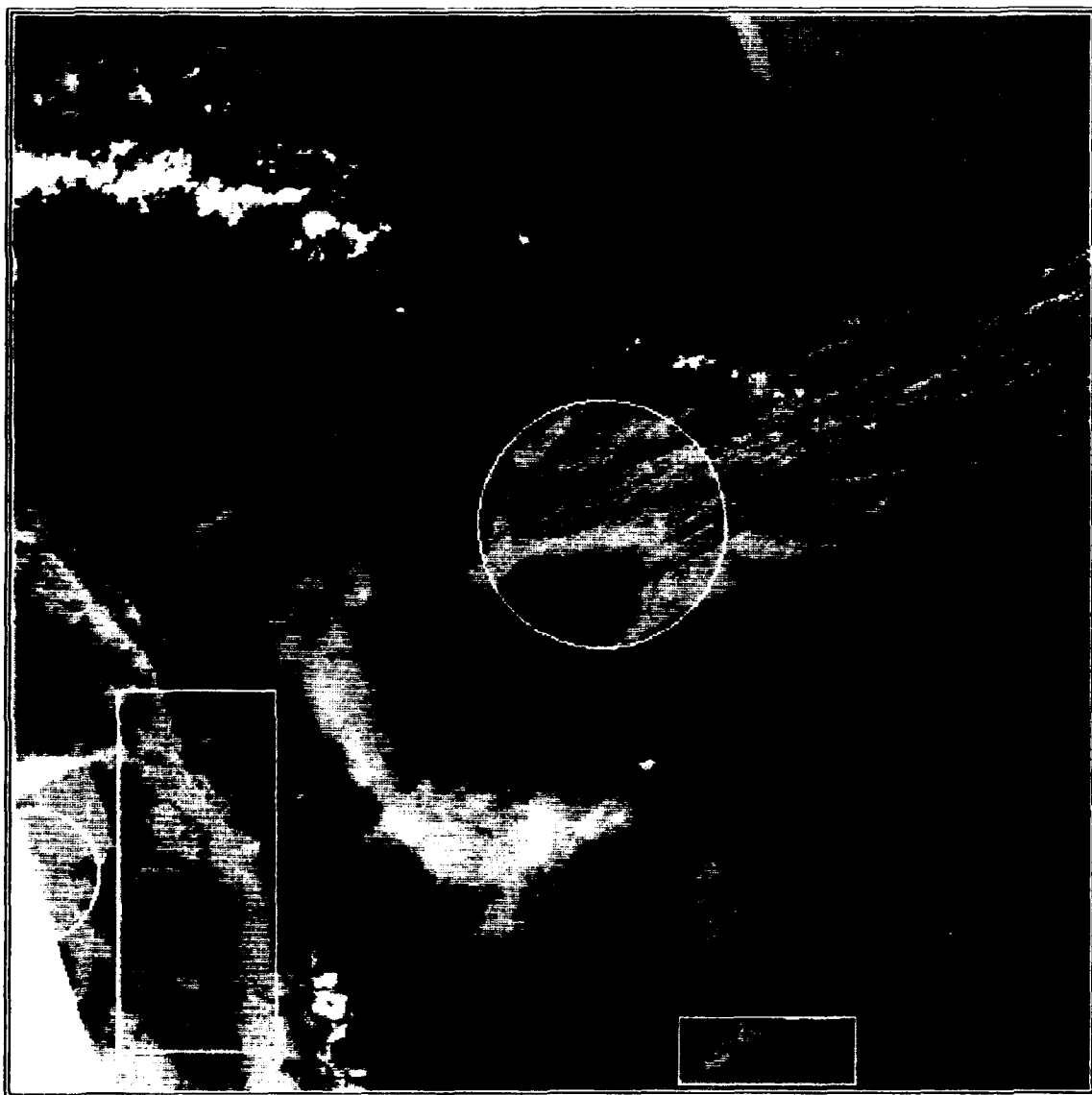


Figure 39. Temp 5 1 March 1991 1026 UTC Arabian Peninsula image. Some clouds (circles) and coastal land (rectangles) have similar brightness temperatures as dust plume.

IMAGE CLASSIFICATION

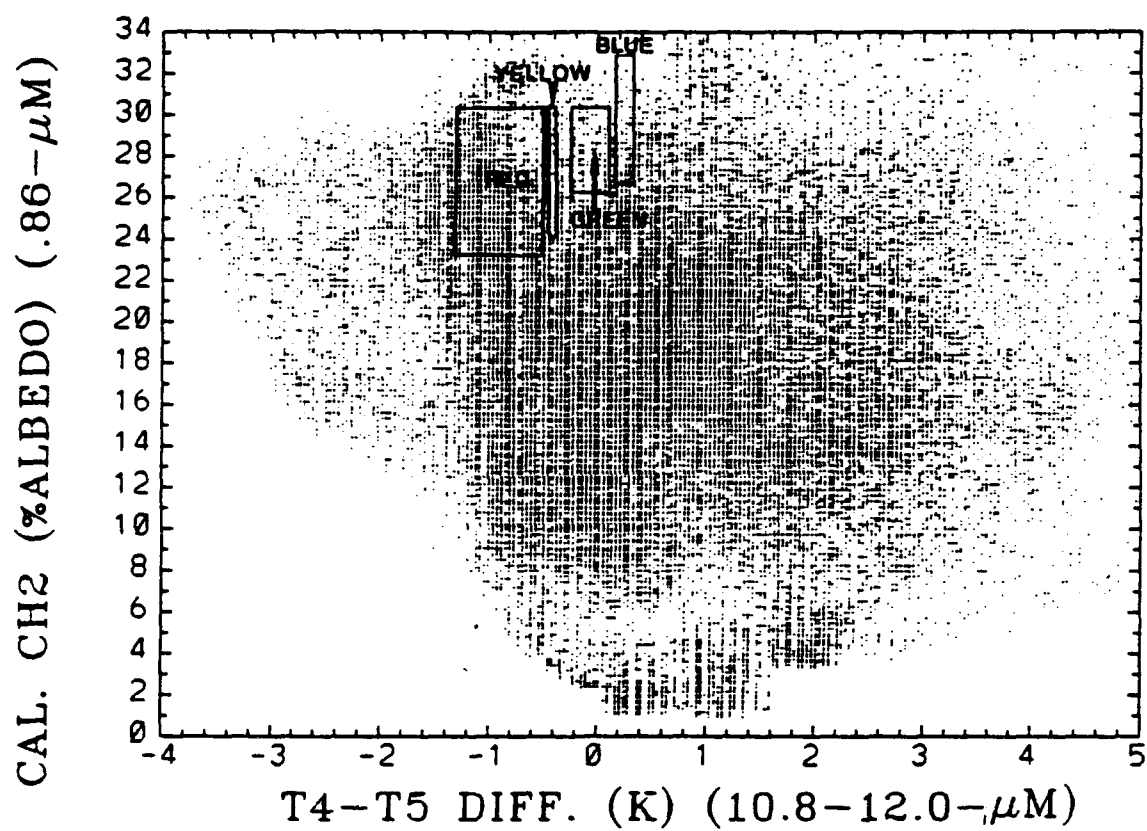


Figure 40. Analyzed 2D "dust" radiative signature for case 4 Arabian Peninsula scatter plot. Colors correspond to those in mask, Figure 41.

of the boxed land area has the same signature as the dust in both images. As in the previous case, this causes some ambiguity with the mask. Figure 43 shows the mask overlaid on the Cal 2 satellite image. The lowest (warmest) dust is in red followed by yellow, green and the highest (coldest) dust in blue. Notice, in fact, much of the boxed land area is masked along with the dust. Thus, once again the dust distribution is depicted but not clearly.

c. T4-T5 versus Temp 4

Figure 44 shows the boxed limits for the dust. Because the dust was clearly separated from the other features it was subdivided into smaller limits so the mask can give better resolution on its distribution. Figure 45 is the mask of this image combination overlaid on the Temp 4 satellite image. Low (warmest) dust is in red followed by orange, yellow, green, blue and the highest (coldest) dust in magenta. The highly discernible dust limits allow this mask to be the most unambiguous representation of the dust plume.

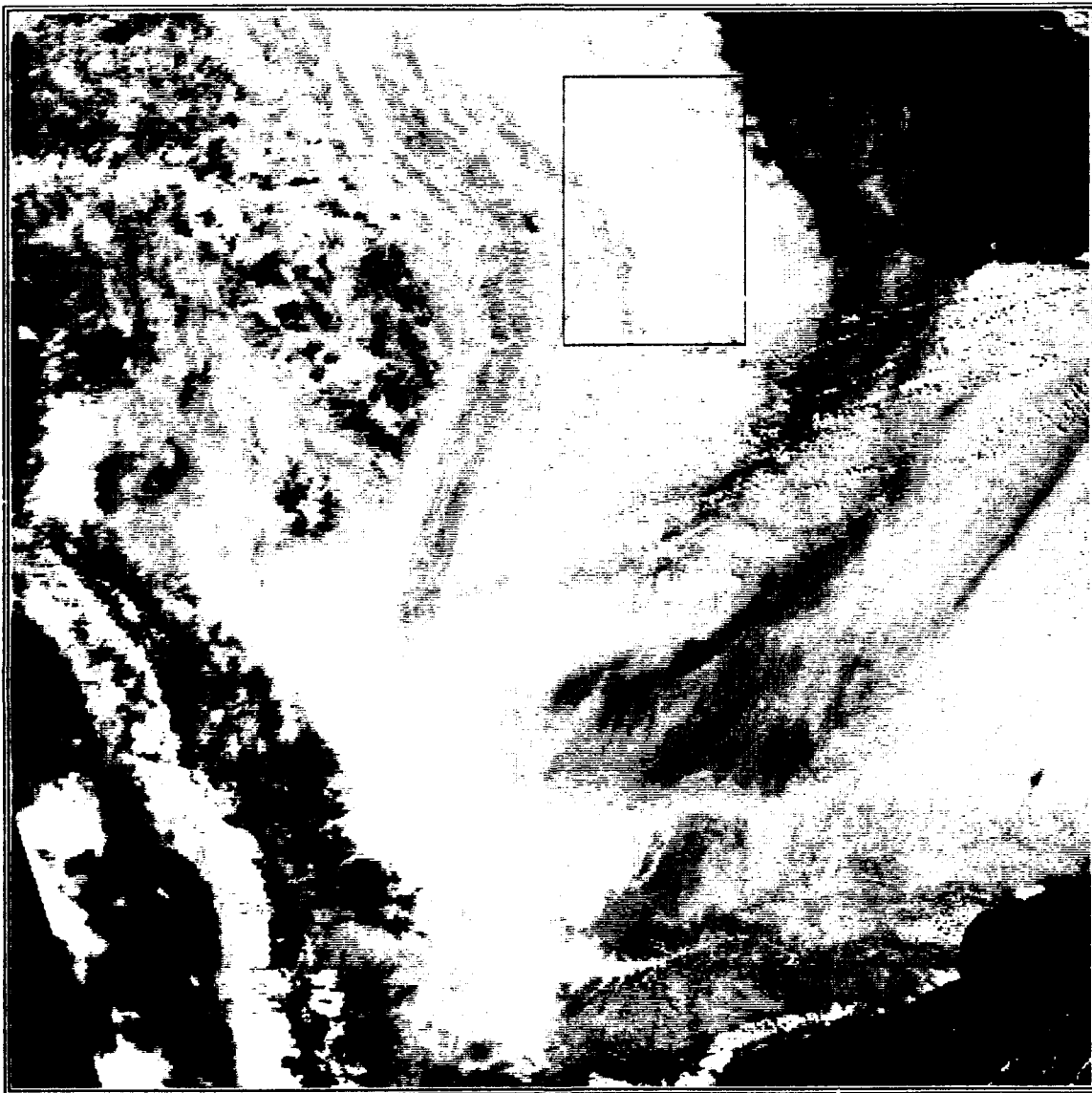


Figure 41. Cal 2 1 March 1991 1026 UTC satellite image. Boxed land area has similar albedo as parts of dust plume.



Figure 42. T4-T5 1 March 1991 1026 UTC satellite image. Boxed land area has similar T4-T5 difference as dust plume.



Figure 43. Cal 2 versus T4-T5 mask utilizing limits in Figure 40. Mask overlaid on Cal 2 image shows approximate dust plume distribution. Note the ambiguity between dust plume and land area in upper right corner.

IMAGE CLASSIFICATION

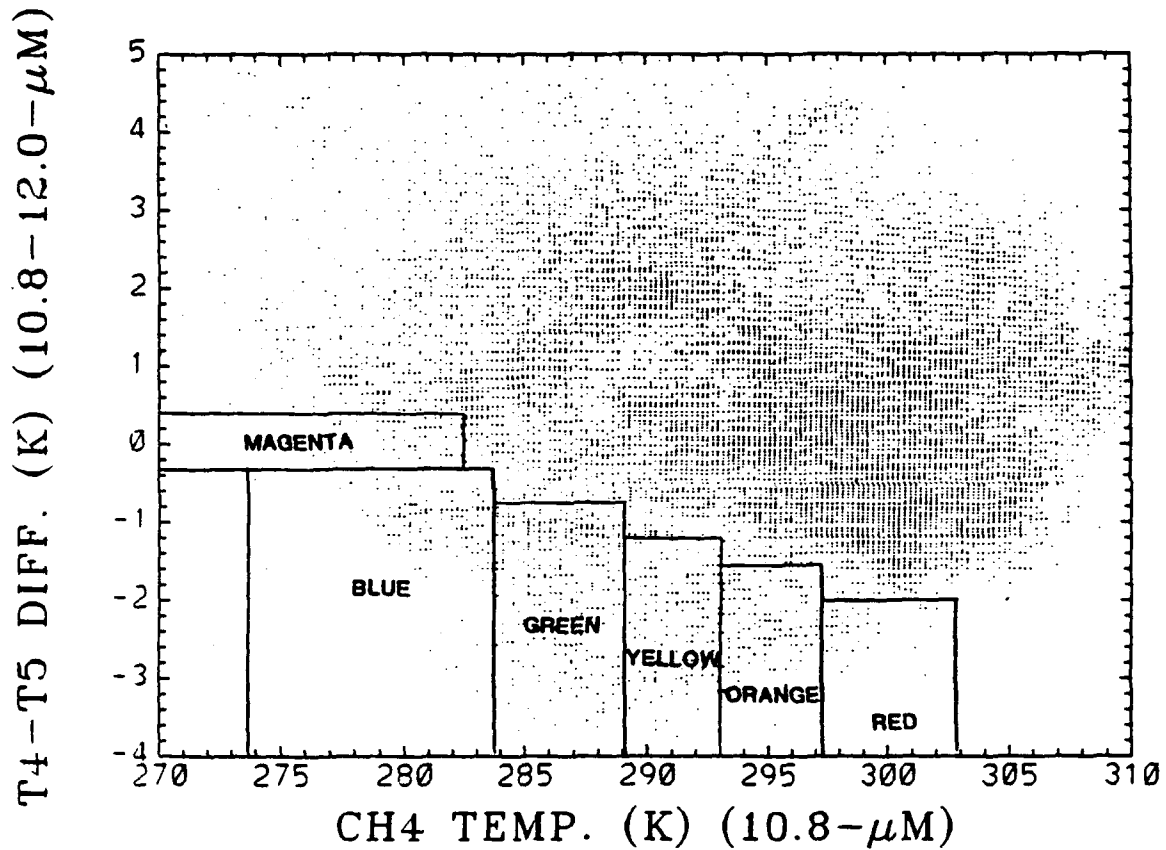


Figure 44. Analyzed 2D "dust" radiative signature for Case 6 Arabian Peninsula scatter plot. Colors correspond to those in mask, Figure 45.



Figure 4b T4-T5 versus Temp 4 mask utilizing limits in Figure 44. Mask overlaid on Temp 4 image shows unambiguous dust distribution. Where red represents the lowest dust and magenta represents the highest dust.

V. CONCLUSIONS AND RECOMMENDATIONS

A. SMOKE RADIATIVE SIGNATURE

The following conclusions have been drawn concerning the smoke radiative signature of smoke. First, smoke detection over water is more difficult than over land. Isolation of the signature is complicated by the low reflectance of both smoke and water in the solar spectrum and relative transparency of smoke at IR wavelengths. The image combination of S12L versus Temp 4 is the best for discerning smoke over water. Contrasting the different absorption characteristics of water between channels 1 and 2 isolates the smoke signature. Second, smoke absorbs the visible spectrum wavelengths equally well (appears black on all visible images). Thus, there is strong contrast with most land regions which makes it relatively easy to detect. Third, smoke particles become more transparent with increasing IR wavelength. This is apparent from image combination of T3-T4 versus Temp 4. Fourth, high atmospheric water content in the presence of smoke particles provides better IR wavelength detection. The smoke particles act as condensation nuclei and allow liquid water drops to form. And finally as smoke thins, its signature becomes more and more characteristic of the underlying surface which complicates its detection as it disperses.

B. DUST RADIATIVE SIGNATURE

There are four main conclusions drawn in this study concerning the dust signature. First dust detection over land is more difficult than over water. Isolation of the aerosol signature is complicated by the influence of the highly diverse land features. Second, dust is highly reflective at visible wavelengths. Third, the dust exhibits a general trend of increasing absorption with IR wavelength. Finally, the strong difference of absorption between channels 4 and 5 allows for the most accurate detection of dust.

C. TWO DIMENSIONAL MASK AND SCATTER PLOT TECHNIQUE

The mask routine uniquely illustrates aerosol spatial distributions using two dimensional radiative limits. It clearly defines detected aerosols in a way that does not "wash out" when reproduced or copied. Since it represents aerosol distributions well, it would be an excellent mission briefing tool.

The scatter plot technique works well in separating and defining aerosol radiative signature limits. Of course, some image/parameter combinations are better than others. But the idea is to find the best combination that contrasts with known characteristics of the aerosol and separates it from the other features as was done in this project.

The scatter plot technique in combination with the mask routine does show promise for possible fleet application.

Granted, there is much more work to be done, but it is conceivable that an algorithm based on these techniques could one day be used for aerosol tracking and mission planning/briefing.

D. RECOMMENDATIONS

The two parameter scatter plot and mask, in certain cases, gave some relatively unambiguous depictions of aerosol distributions. Investigation of a three parameter scatter plot/mask routine, however, is recommended. Three parameters should further enhance aerosol signature detection. As an example, unique smoke characteristics are represented in S12L, Temp 4 and T3-T4 parameters. Analysis in all three, simultaneously, would allow even more unambiguous signature separation than is currently attained relying on just two parameters.

It is recommended to build upon the combination of the scatter plot analysis technique and masking routine to devise an aerosol detection algorithm. As implied previously, such an algorithm could have military application.

This project was conducted using a single day case study. The masking limits analyzed for the aerosols in this project are most likely only valid for 1 March 1991. Therefore, it is recommended that additional cases be examined to further verify the techniques used in this project and to study geometry and temperature variation effects.

Finally, it is recommended that future AVHRR radiometers have a higher upper end channel 3 wavelength limit. The current limit does not allow "hot" objects greater than approximately 322° K to be discerned. This is a result of not accounting for the effect of solar reflectance on channel 3 brightness temperatures.

LIST OF REFERENCES

- Carlson, T.N., and S.G. Benjamin, 1980: Radiative heating rates for Saharan dust. *J. Atmos. Sci.* 37, 193-213.
- Crutzen, P.J., I.E. Galbally, and C. Bruhl, 1984: Atmospheric effects from post-nuclear fires. *Clim. Change*, 6, 323-364.
- Durkee, P.A. 1984: The relationship between marine aerosol particles and satellite detected radiance. Ph.D. Thesis, Colorado State University, Fort Collins, CO, US ISSN 0067-0340, 124 pp.
- Johnson, D.W., C.G. Kilsby, D.S. McKuna, R.W. Saunders, G.J. Jenkins, F.B. Smith and J.S. Foot, 1991: Airborne observations of the physical and chemical characteristics of the Kuwait oil smoke plume. *Nature*, 353, 617-621.
- Kidder, S.Q. and T.H. Vonder Haar, 1992: Introduction to satellite meteorology. In preparation Academic Press.
- Limaye, S.S., V.E. Suomi, C. Velden and G. Tripoli, 1991: Satellite observations of smoke from oil fires in Kuwait. *Science*, 252, 1536-1538.
- Taha, M.F., S.A. Harb, M.K. Nagib, and A.H. Tantany, 1981: *The Climate of the Near East*. IN World Survey of Climatology. vol 9. Ed. K. Takahashi and H. Arakawa. Elsevier Scientific Publishing Company, Amsterdam, Netherlands, 333 pp.
- Turco, R.P., O.B. Toon, T.P. Ackerman, J.B. Pollack, C. Sagan, 1990: Climate and smoke: an appraisal of nuclear winter. *Science*, 247, 166-175.
- USS Wisconsin (BB 64), Report 3140-5, *Oceanographic Post-Deployment Report for the Period 07 August 1990 to 28 March 1991*, by D.S. Bill III, encl. 1, pp. 5-6, 29 April 1991.

INITIAL DISTRIBUTION LIST

1. Defense Technical Information Center 2
Cameron Station
Alexandria, VA 22304-6145
2. Library, Code 52 2
Naval Postgraduate School
Monterey, CA 93943-5000
3. Chairman (Code OC/Co) 1
Department of Oceanography
Naval Postgraduate School
Monterey, CA 93943-5000
4. Chairman (Code MR/Hy) 1
Department of Meteorology
Naval Postgraduate School
Monterey, CA 93943-5000
5. Philip A. Durkee, Code MR/De 1
Department of Meteorology
Naval Postgraduate School
Monterey, CA 93943-5000
6. LCDR William P. Morgan 1
Helicopter Combat Support Squadron Five
U.S. Naval Air Station
FPO San Francisco, CA 96637-2714
7. Commander 1
Naval Oceanography Command
Stennis Space Center
MS 39529-5000
8. Commanding Officer 1
Naval Oceanographic Office
Stennis Space Center
MS 39522-5001
9. Commanding Officer 1
Fleet Numerical Oceanography Center
Monterey, CA 93943-5005

- | | | |
|-----|---|---|
| 10. | Commanding Officer
Naval Oceanographic and Atmospheric
Research Laboratory
Stennis Space Center
MS 39529-5004 | 1 |
| 11. | Director
Naval Oceanographic and Atmospheric
Research Laboratory
Monterey, CA 93943-5006 | 1 |
| 12. | Chief of Naval Research
800 N. Quincy Street
Arlington, VA 22217 | 1 |
| 13. | Tom Lee
Naval Research Laboratory
Monterey, CA 93943-5006 | 1 |